AD-751 182

# FLUERICS: 33. DESIGN AND STAGING OF LAMINAR PROPORTIONAL AMPLIFIERS

Francis M. Manion, et al

Harry Diamond Laboratories
Washington, D. C.

September 1972

DA-1T061102A33B
AMCMS Code: 611102.11.71200
HDL Proj: 302231

HDL-TR-1608

# FLUERICS: 33. DESIGN AND STAGING OF LAMINAR PROPORTIONAL AMPLIFIERS

by

Francis M. Manion

George Mon

September 1972





U.S. ARMY MATERIEL COMMAND
HARRY DIAMOND LABORATORIES
WASHINGTON, D.C. 20438

The findings in this report are not to be construed as an official Department of the Army position unless so designated by other authorized documents.

Citation of manufacturers' or trade names does not constitute an official indorsement or approval of the use thereof.

Destroy this report when it is no longer needed. Do not return it to the originator.

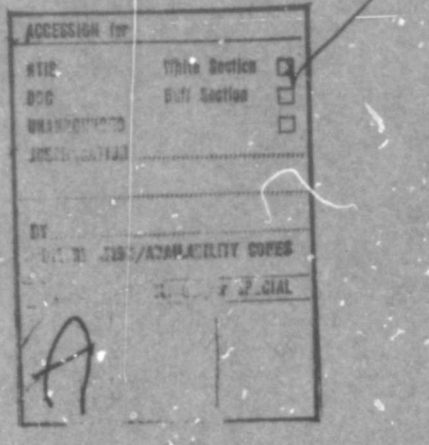

UNCLASSIFIED

Security Classification

## DOCUMENT CONTROL DATA - R & D

*(Security classification of title, body of abstract and indexing annotation must be entered when the overall report is classified)*

1. ORIGINATING ACTIVITY *(Corporate author)*

Harry Diamond Laboratories
Washington, D.C. 20438

2a. REPORT SECURITY CLASSIFICATION

Unclassified

2b. GROUP

3. REPORT TITLE

FLUERICS 33: DESIGN AND STAGING OF LAMINAR PROPORTIONAL AMPLIFIERS

4. DESCRIPTIVE NOTES *(Type of report and inclusive dates)*

5. AUTHOR(S) *(First name, middle initial, last name)*

Francis M. Manion and George Mon

6. REPORT DATE

September 1972

7a. TOTAL NO. OF PAGES

56 44

7b. NO. OF REFS

3

8a. CONTRACT OR GRANT NO.

b. PROJECT NO. DA-1T061102A33B

c. AMCMS Code: 611102.11.71200

d. HDL Proj: 302231

9a. ORIGINATOR'S REPORT NUMBER(S)

HDL-TR-1608

9b. OTHER REPORT NO(S) *(Any other numbers that may be assigned this report)*

10. DISTRIBUTION STATEMENT

Approved for public release; distribution unlimited.

11. SUPPLEMENTARY NOTES

12. SPONSORING MILITARY ACTIVITY

U.S. Army Materiel Command

13. ABSTRACT

This report discusses the design and staging of a laminar flueric proportional amplifier with a pressure gain greater than 15, a dynamic range of over 1000, and a bandwidth ranging from 100 to 1000 Hz depending on the supply pressure. By scaling with Reynolds number based on channel depth, several of these elements have been connected in series to form a three-stage, open-loop gain block with a pressure gain greater than 1000, a dynamic range of over 400, and a bandwidth greater than 100 Hz. The output of the amplifier itself and of the gain block has a flat saturation characteristic.



DD FORM 1 NOV 68 1473 REPLACES DD FORM 1473, 1 JAN 64, WHICH IS OBSOLETE FOR ARMY USE.

UNCLASSIFIED

Security Classification

| 14. KEY WORDS | LINK A | | LINK B | | LINK C | |
|---|---|---|---|---|---|---|
| | ROLE | WT | ROLE | WT | ROLE | WT |
| Proportional amplifier | 8 | 3 | | | | |
| Gain block | 8 | 3 | | | | |
| Staging | 8 | 3 | | | | |
| Frequency response | 8 | 3 | | | | |
| Pressure gain | 8 | 3 | | | | |
| Power gain | 8 | 3 | | | | |
| Flow gain | 8 | 3 | | | | |

AD

HDL-TR-1608

# FLUERICS: 33. DESIGN AND STAGING OF LAMINAR PROPORTIONAL AMPLIFIERS

by

Francis M. Manion

George Mon

September 1972

U.S. ARMY MATERIEL COMMAND

HARRY DIAMOND LABORATORIES

WASHINGTON, D.C. 20438

## ABSTRACT

This report discusses the design and staging of a laminar flueric proportional amplifier with a pressure gain greater than 15, a dynamic range of over 1000, and a bandwidth ranging from 100 to 1000 Hz depending on the supply pressure. By scaling with Reynolds number based on channel depth, several of these elements have been connected in series to form a three-stage, open-loop gain block with a pressure gain greater than 1000, a dynamic range of over 400, and a bandwidth greater than 100 Hz. The output of the amplifier itself and of the gain block has a flat saturation characteristic.

## CONTENTS



TABLES



FIGURES

## 1. INTRODUCTION

Kirshner and Manion[1] describe the development of the jet deflection proportional amplifier during the past eleven years. They show that the development of a useful fluidic amplifier is a complex task and point out some of the many unknowns that limit the further refinement of this type of amplifier. The references quoted in that paper provide a source of papers describing amplifier development.

Silhouettes of commercially available jet-deflection amplifiers discussed in that ASME paper are shown in figure 1. All of these amplifiers were experimentally developed to operate in the turbulent flow regime and consequently have a limited dynamic range. The dynamic range achievable with these devices varies from 100 to 500 at bandwidths of 500 to 25 Hz, respectively. The jet deflection amplifier's dynamic range must be improved to make it useful to system designers.

It was immediately apparent when we began this investigation that laminar proportional amplifiers were necessary to increase dynamic range. In our research, we found that NASA (Langley) had adapted a pressure field proportional amplifier (originally developed for turbulent operation) to the laminar flow regime. The original amplifier was developed by Griffin and Gebben.[2] As originally developed (fig. 2), it had a flat saturation characteristic and operated at Reynolds numbers greater than 2360 based on element depth. It had a dynamic range of 100 for a 20-Hz bandwidth and a staged pressure gain of about 4 to 5 per stage, but the authors noted that its performance was limited by zero shifts and gain variations that were caused by pressure level changes in the control ports.

R.F. Hellbaum of NASA (Langley) used this amplifier design as a starting point in development of a low Reynolds number proportional amplifier. He obtained pressure gains of 8 to 10 per stage at Reynolds numbers (for square nozzles) of 1000 to 1800. However, the gain decreased as the bias control level increased, resulting in low staging gain. He overcame this effect by a vent pressure level control. With this control and many geometrical changes, Hellbaum has staged five amplifiers to obtain a pressure gain of 2400 (4.744 per stage).

An important result of NASA's laminar amplifier work is that their preliminary data showed that blocked output pressure gain of 8 to 10 can be achieved with a dynamic range of 500 to 1000 for a bandwidth of 20 Hz.

These results encouraged us to concentrate our effort on developing a laminar proportional amplifier. Our development was successful and has resulted in a three-stage laminar gain block that has a pressure gain greater than 1000, a dynamic range greater than 400, and a bandwidth greater than 100 Hz.

As part of our effort, we performed experiments to define the operating Reynolds number range for laminar jet deflection amplifiers and developed a staging method to assure maximum dynamic range. This report discusses these results as well as the cause of and a proposed solution to the bias level sensitivity problem.

---

[1] Kirshner, J.M. and Manion, F.M., "The Jet Deflection Proportional Amplifier," ASME Paper No. 70-Flcs-17, presented at 10th Anniversary Fluidics Conference, Atlanta, Ga., June 1970.

[2] Griffin, W.S. and Gebben, V.D., "A Proportional Fluid Jet Amplifier with Flat Saturation Characteristics and its Application to Gain Block," NASA TM X-1915, November 1969.

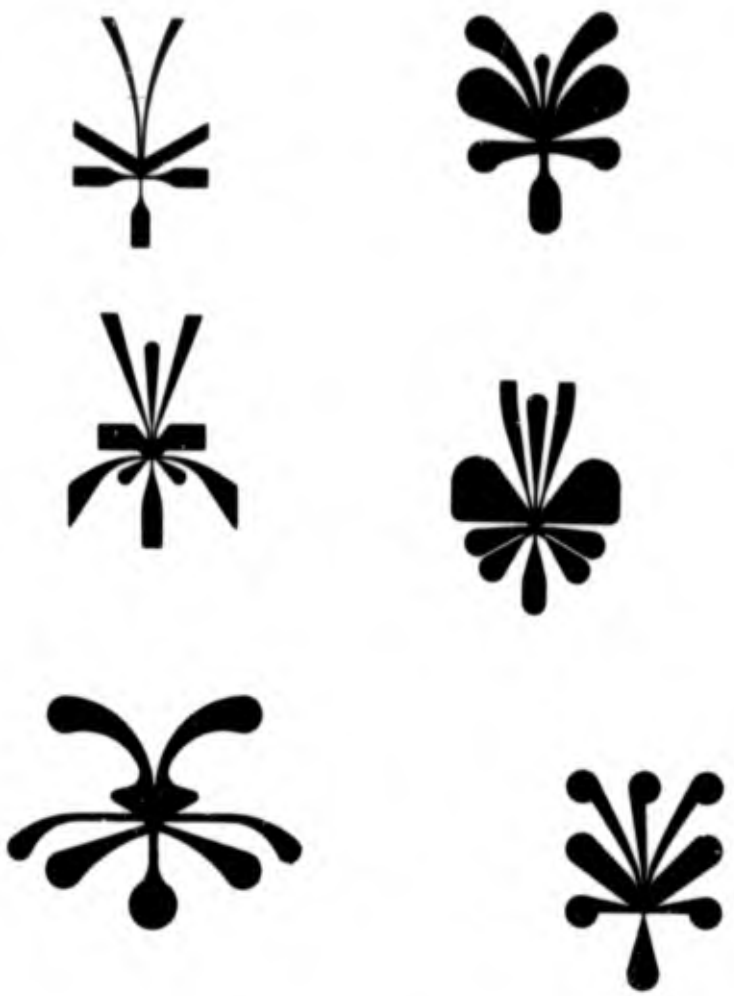

Figure 1. Silhouettes of commercially available proportional amplifiers.

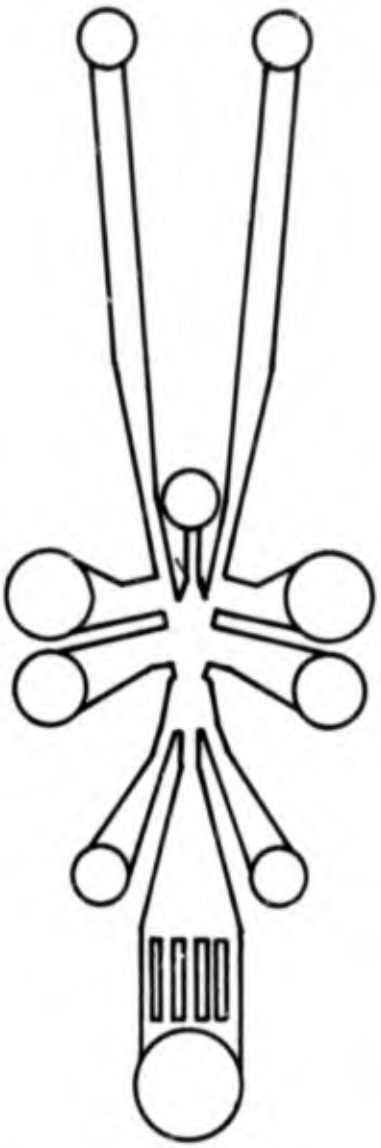

Figure 2. Schematic of Griffin-Gebben (NASA) turbulent proportional amplifier.

In addition, a theoretical discussion of the dynamic response of the amplifier is given and future work needed to make the element useful to the system engineer is outlined.

## 2. LAMINAR JET AMPLIFIER CONFIGURATION AND CHARACTERISTICS

The shape of the laminar proportional amplifier is given in figure 3. This design overcomes the pressure sensitivity to bias level by a geometrical change in the control nozzle structure and by properly staging the supply pressures. The amplifier has single-stage pressure gain greater than 15 (fig. 4), good saturation characteristics, and low noise.



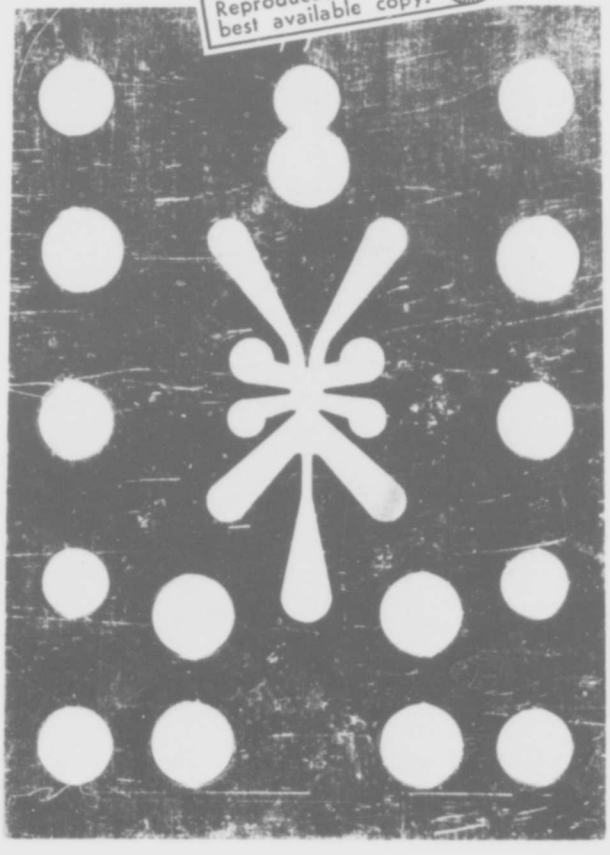

Figure 3. Photograph of present design of laminar proportional amplifier.

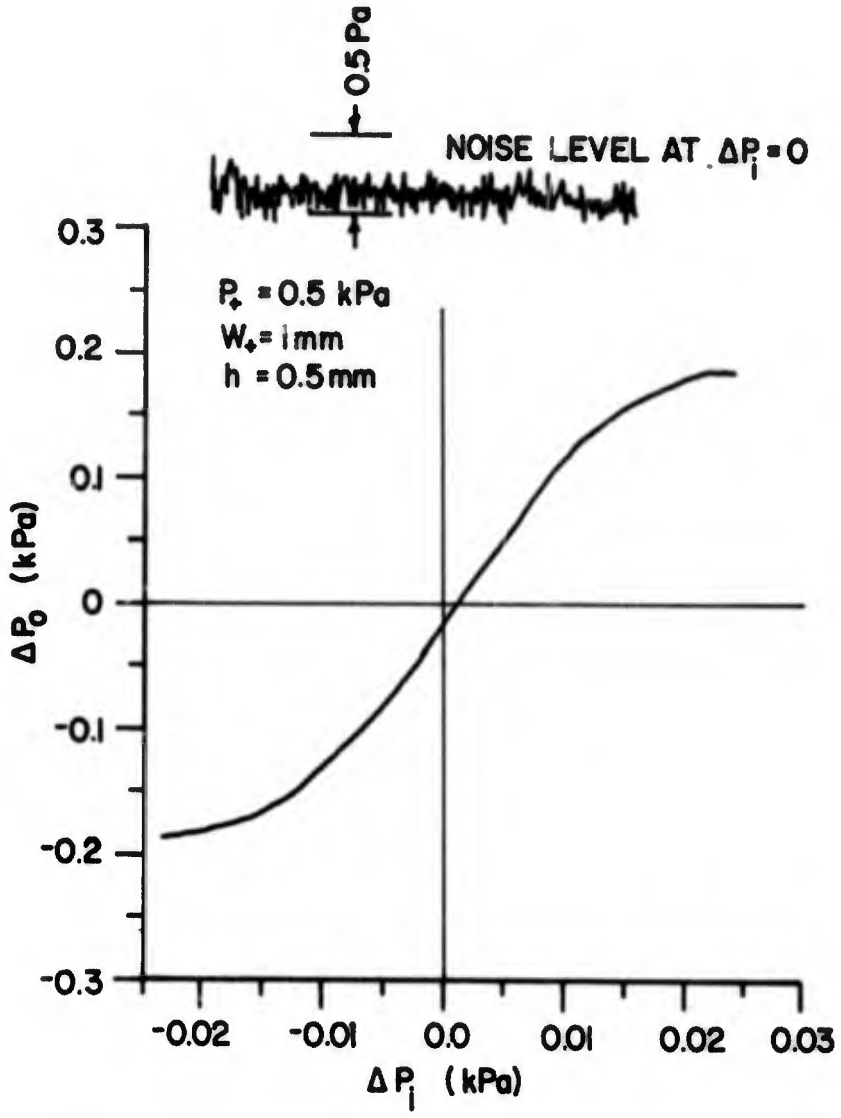


Figure 4. Single-stage pressure gain and dynamic range.

The element was designed so that the input is isolated from the output loading. In figure 5, the input characteristic has been recorded for an undeflected supply jet (no difference between input control pressures). The characteristic is shown for blocked and fully open output areas. The characteristics are identical except in the negative pressure range, which is not used in staged amplifiers. This shows that the input characteristic is decoupled from the output load. The characteristic is also rather linear over an appreciable range, which simplifies the analysis. The need to operate these amplifiers so as to have the same interaction region flow field in all element stages cannot be overemphasized if these are staged for large dynamic range and a smooth gain curve.

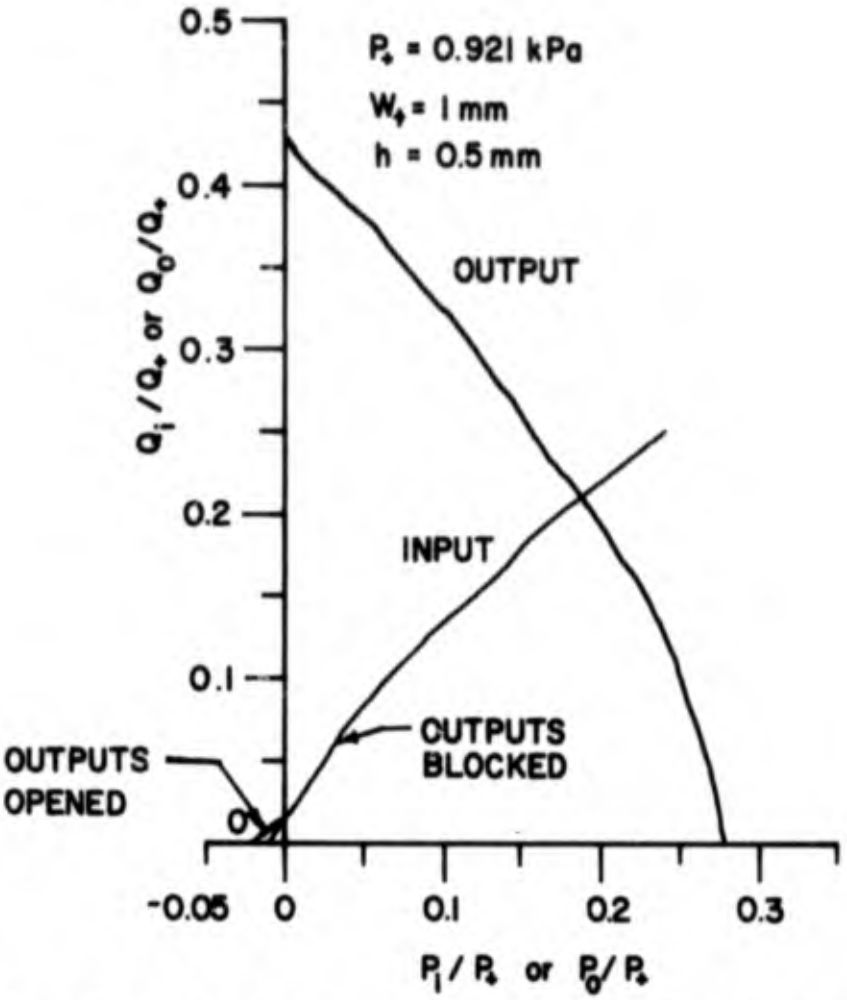


Figure 5. Input and output pressure-volume flow characteristic.

The dynamic range of this particular element is greater than 1200 for a bandwidth of 20 Hz, which is the bandwidth of our recording instrument. The actual recorded data are shown in figure 4. Additional measurements with wider bandwidth instruments are being taken, but results are not yet available.

The design of a pressure field laminar jet deflection amplifier rather than a momentum exchange design has resulted in a significant increase in dynamic range, even though the lack of supply flow conditioning (i.e., regulation of the input flow and the effects of the ambient testing environment) still limits the results. Our visualization study on a large amplifier model shows that a pressure field effectively deflects the laminar jet without disturbing its flow field; but for the same jet deflection, a momentum interaction design introduces noise. Although our results show the pressure field approach to be very effective for laminar designs, it creates more noise in turbulent flow because of the unsteadiness of the entrained shear layer near the downstream edge of the control nozzle structure. In turbulent flow, the momentum exchange design appears less noisy.

The steadiness of laminar flow shows great potential for an even larger dynamic range for this type amplifier. More important, laminar flow can be scaled; therefore, large scale models can be used effectively for design and testing and the results can be used to build amplifiers of a size for use with any fluid. For example, an element using this design has been tested using hydraulic oil. Its gain characteristic is shown in figure 6. The element was also tested with air at the same Reynolds number and it has a similar gain characteristic. This result is very important, since it shows that our designs are not limited to the working fluid in which they were tested.

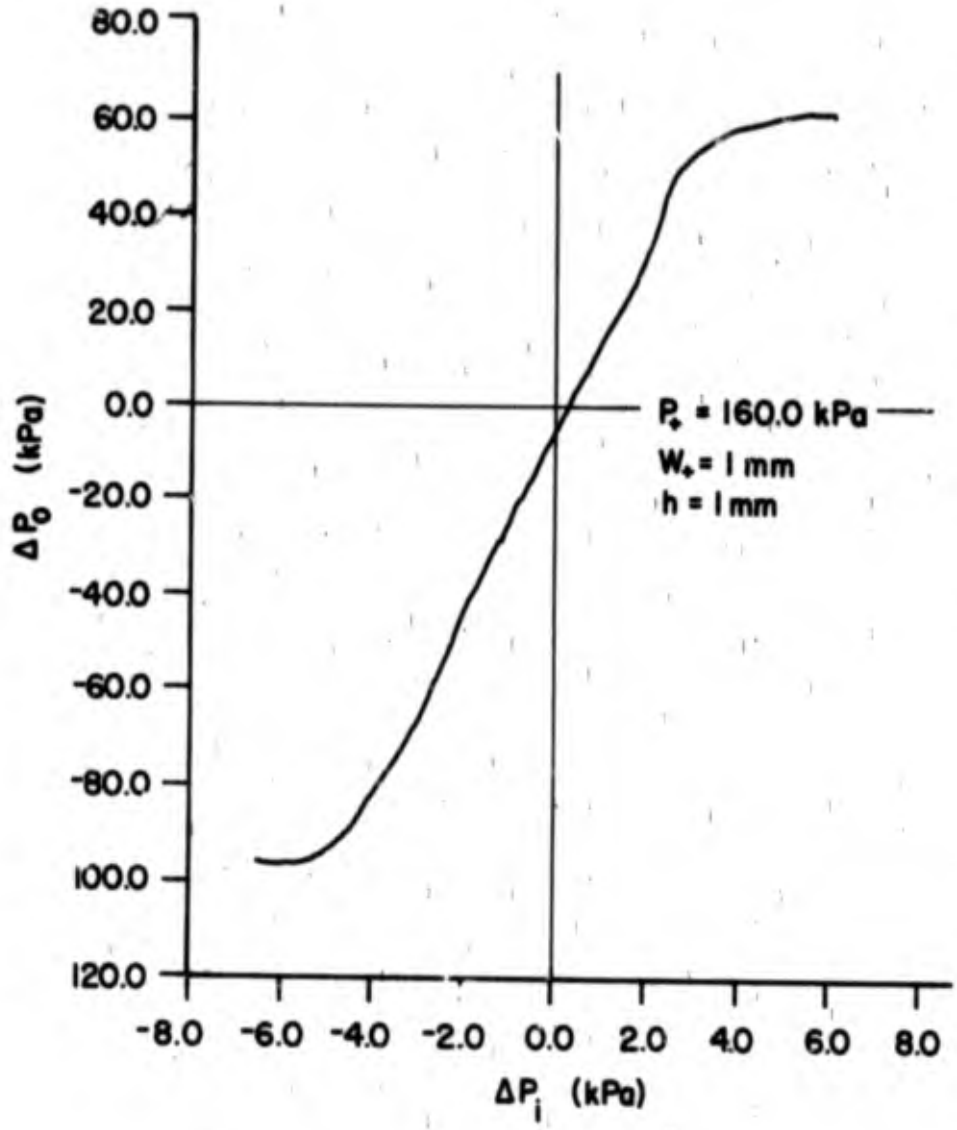


Figure 6. Single-stage pressure gain of laminar proportional amplifier operating in oil.

## 3. REYNOLDS NUMBER RANGE FOR LAMINAR JET AMPLIFIERS

In laminar flow elements, the Reynolds number describes the flow similarity between similar units; consequently the proper definition of a laminar flow field Reynolds number is essential if experimental results are to be compared and models scaled. For this reason, an experiment was conducted to determine the characteristic dimension of the laminar amplifier's flow field. The element depth was chosen as the parameter to be studied, because laminar free jets do not normally exist at Reynolds numbers of 1000 to 2000, indicating that the influence of the top and bottom plates must be important. (Griffin and Gebben[2] also used channel depth as the characteristic dimension in their definition of the Reynolds number although no justification was given.) The experiment was performed using a commercially available laminated proportional amplifier made with 0.1-mm-thick stainless steel laminas. By stacking these laminas, proportional amplifiers were made in depths in multiples of 0.1 mm. The amplifier's blocked output pressure gain was measured for each element depth. Figure 7 shows a plot of the pressure gain as a function of Reynolds number (Re) which is based on channel depth. The data show that if the Reynolds number is based on channel depth, the pressure gain versus Reynolds number gives essentially a single curve, indicating that the channel depth is a meaningful characteristic dimension. Similar tests were performed on the laminar proportional elements of HDL (Harry Diamond Laboratories) design, and the same definite trend was noted.

The choice of this characteristic dimension (depth) appears logical since the amplifiers have channel depths much smaller than their plan view dimensions except at the nozzle exit. For the most part, the flow field is developing and the depth is the characteristic dimension. If fully developed Poiseuille flow existed in the amplifier, then the scaling dimension would have been based on depth squared divided by the downstream distance as in Hele-Shaw flow. In the internal flow field of the amplifier, the depth velocity profile is developing; but since the data indicate that the channel depth rather than depth square is the characteristic dimension, the essential parts of the flow field are not fully developed in the depth dimension

The aspect ratio of the nozzle influences the operating Reynolds number range as does the condition of the supply flow. However, for aspect ratios under unity, the depth appears to be of primary influence and is thus the characteristic dimension.

Tests conducted on our elements have shown that a suitable operating Reynolds number range for an aspect ratio of unity or less is 700 to 1800. Test results on elements with aspect ratios of 2.0 and 1.5 also followed the same trend, but it is reasonable to assume that as the aspect ratio becomes greater than unity, the use of the depth dimension as the characteristic length is less accurate.

Figure 8 shows photographs of a large scale water model (earlier design configuration) using dyed supply jets having Reynolds numbers of 300, 975, and 2150. Since the jet shown (fig. 8b) operating at a Reynolds number in the proper range (975) is very quiet, amplifiers operating with kind of jet flow should have a large dynamic range potential.

The Reynolds number range is limited by surface shear and by transition to turbulence. At lower Reynolds numbers, shear losses from the top and bottom plates reduce signal gain (for this plan view structure)

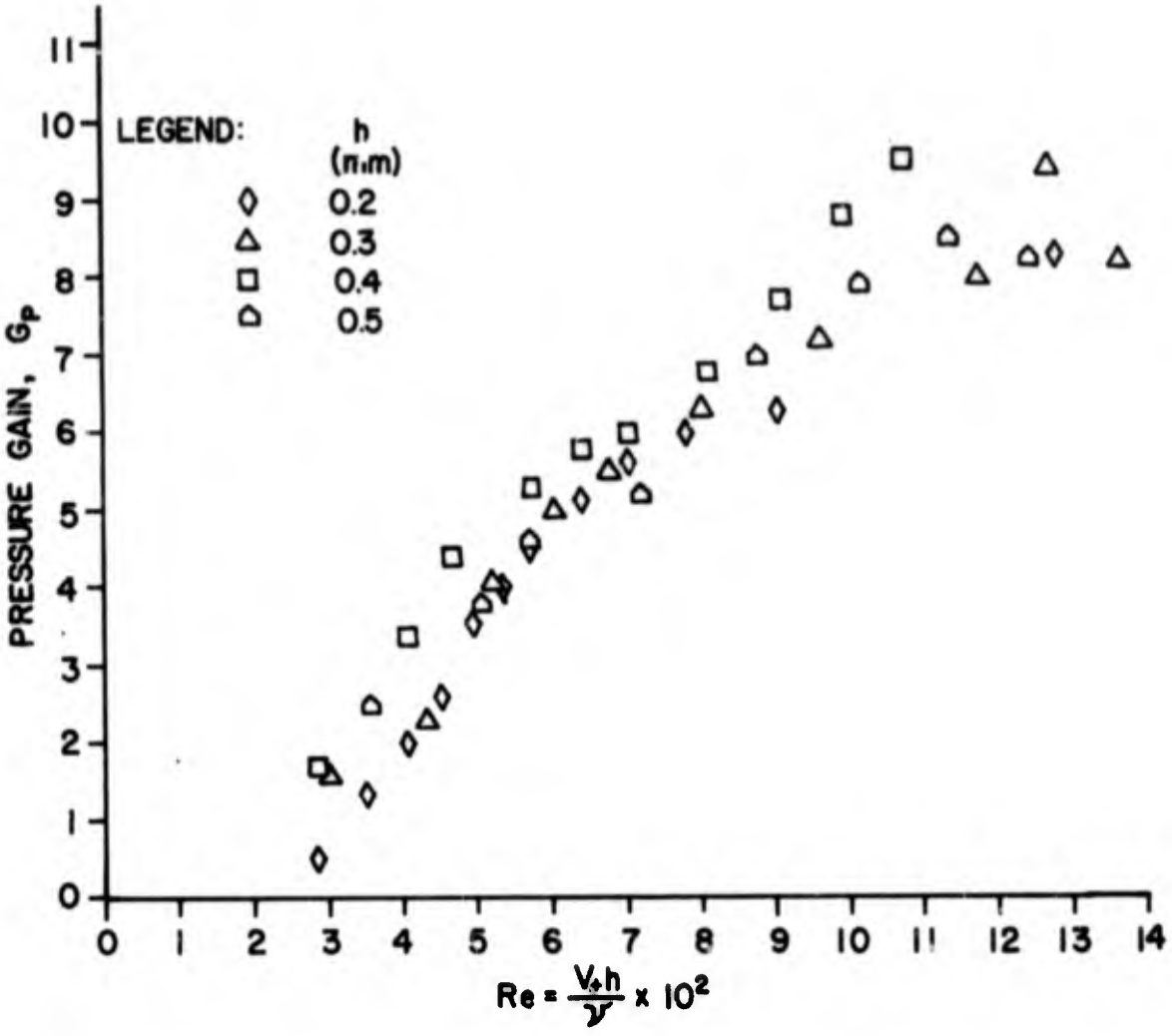


Figure 7. Variation of pressure gain versus Reynolds number with channel depth h as the characteristic dimension.

by forcing the jet to spread as shown in figure 8a and diminishing its centerline velocity. At higher Reynolds numbers, turbulence is encountered in the flow, as shown in figure 8c. This is evidenced by a large increase in eddying visible in the photograph. From these photographs, an estimate of the operating Reynolds number range for the proper laminar amplifier operation can be obtained.

Pressure measurements made in the control nozzle chamber (with blocked inputs) show that the control pressure is positive at very low supply pressures for an element configuration such as that of figure 3. This implies that the flow at the jet edge spills back into the control nozzle chamber. As the supply pressure is increased, this positive pressure reaches a maximum value and then gradually decreases, becoming negative. The Reynolds number at which the blocked input control pressure is zero varies depending on nozzle design and is a subject for more research.

(a) Re = 300 (b) Re = 975 (c) Re = 2,150

Figure 8. Variation of jet flow characteristics with Reynolds number, $v_+h/\nu$.

This approximate definition of the proper operating Reynolds number range can be used with different element depths to define an operating supply pressure region for laminar jet amplifiers as is shown in figure 9. Element depths of 0.1 to 2 mm were arbitrarily selected. For the minimum and maximum depths shown in figure 9, the ratio of maximum to minimum supply pressure is 2500. For maximum dynamic range, the power supplies of each successive stage must be increased by the factor of the pressure gain so that all elements saturate simultaneously. From figure 9, the last stage to first stage power supply ratio is the gain of n - 1 stages. Therefore, for maximum dynamic range, the total gain possible is 2500 times the gain per stage, or 25,000 if the single stage gain is 10. If more pressure gain per stage is required, the element depth limits must be increased or the dynamic range of the staged amplifier must be reduced. Operation below the proper Reynolds number range is inefficient even though some gain could be obtained.

The definition of an operating range for laminar amplifiers is a significant accomplishment; fluid devices can now be staged, scaled, tested, and analyzed in detail. Also, the problem of building staged amplifiers is greatly simplified, since the decoupled amplifiers operate with one flow field, and this flow field operates properly within a selected Reynolds number range.

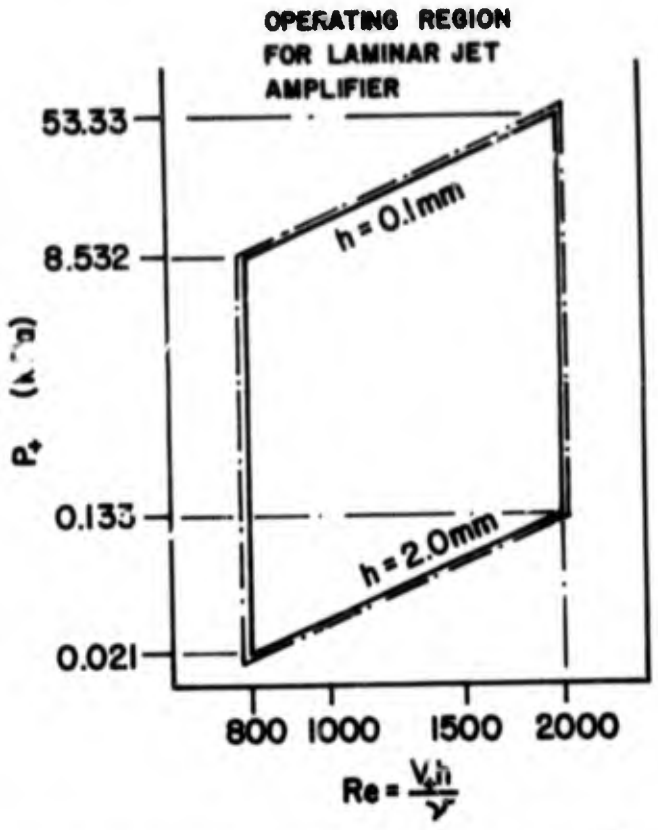


Figure 9. Variation of supply pressure $P_+$ versus Reynolds number with channel depth as a parameter.

## 4. STAGING OF AMPLIFIERS

Two significant factors are used in our staging of laminar proportional amplifiers. The first is the use of output decoupling, and the second is the determination of the Reynolds number range for proper amplifier operation.

The use of decouplers has effectively isolated the amplifier's internal flow field from low frequency downstream load variations. They permit the component designer to concentrate on developing the most efficient receiver arrangement and to set the operating point without worrying about the effect of the next stage.

The determination of a Reynolds number range for amplifier operation permits particular elements to be designed for each operating stage. Particular elements for each stage are necessary to maximize the staged dynamic range and to reduce pressure gain sensitivity to control bias level. For example, if every amplifier is operated from its threshold level to its saturation level, the full dynamic range of a staged gain block is being used. To accomplish this ideal staging, the power supply pressure of successive stages must be increased by the factor of the pressure gain of each stage. This means that if each is 10, the power supply pressure for each succeeding stage should be increased by a factor of 10 to maximize the staged amplifier's dynamic range.

Amplifiers can be built to operate in the proper Reynolds number range with increasing supply pressures by decreasing the depth of each succeeding stage as described previously. A reduced dynamic range can be illustrated by assuming that identical amplifiers were staged using the same supply pressure to each stage. A small deflection of the first stage's jet stream would cause the last stage's jet stream to be deflected to saturation. Therefore, only a small part of the first amplifier's dynamic range is being used. Of course, if the later stages increased in size, this effect could be avoided; but the fabrication of the same element plan view configuration is more economical.

In developing amplifier staging criteria, the designer has several options. Elements can be staged using an identical plan view structure, or the elements can be increased in plan view size. The amplifier's operating Reynolds number can be held constant for all stages or increased in the allowable Reynolds number range. Finally, amplifiers can be staged for maximum pressure gain, maximum flow gain, or maximum power gain.

In order to discuss these designs, two alternative relationships are defined. These are the definitions of Reynolds numbers and input-to-output admittance ratios of these amplifiers.

The Reynolds number is defined as

$$Re = \frac{V_+ h}{\nu} \tag{1}$$

where

$V_+$ = the average supply jet velocity (m/s)

$h$ = element depth (m)

$\nu$ = kinematic viscosity ($m^2/s$)

This can be written as

$$Re \propto h\sqrt{P_+} \tag{2}$$

where

$P_+$ = supply jet pressure (kPa)

It should be noted, as was discussed in detail earlier, that the Reynolds number is based on the fluidic element's depth. Experiments have shown that operating range of these proportional fluidic amplifiers is in the Reynolds number range of 700 to 1800.

The input-to-output admittance ratio is important to assure that the staged elements will have a maximum dynamic range. The pressure gain available to the next stage must be used to determine the supply pressure of the next element. The staging efficiency can be written as

$$G_p \left( \frac{R_{i,n+1}}{R_{i,n+1} + R_{o,n}} \right) = G_p \left( \frac{Y_{o,n}}{Y_{o,n} + Y_{i,n+1}} \right) = \frac{P_{+,n+1}}{P_{+,n}} \tag{3}$$

where

$G_p$ = elements' pressure gain for blocked output area

$R$ = resistance

$Y_{o,n} = \frac{1}{R_{o,n}}$ = output admittance for the n-th stage [$m^3/(kPa\text{-}s)$]

$Y_{i,n+1} = \frac{1}{R_{i,n+1}}$ = input admittance for the n+1 stage [$m^3/(kPa\text{-}s)$]

$P_{+,n}$ = supply pressure for the n-th stage (kPa)

$P_{+,n+1}$ = supply pressure for the n+1 stage (kPa)

This admittance ratio $[Y_{o,n}/(Y_{o,n} + Y_{i,n+1})]$ is important if these elements are to be staged for dynamic range. If the admittance is defined for zero frequency, using orifice relations, the supply admittance can be written as

$$Y_+ = \frac{2(w_+h)^2}{\rho Q_+} \tag{4}$$

where

$Y_+$ = admittance of the supply nozzle [$m^3/(kPa\text{-}s)$]

$w_+$ = supply nozzle width (m)

$h$ = supply nozzle depth (m)

$\rho$ = fluid density [$(kPa\text{-}s^2)/m^2$]

$Q_+$ = supply flow ($m^3/s$)

If $Y_i$ and $Y_o$ of a given element are normalized to $Y_+$ (the supply admittance), then by comparing supply admittances from stage to stage, a comparison of input or output admittances from stage to stage can be made. Defining $Y_{+,n+1}$ in terms of $Y_{+,n}$ and assuming incompressible flow

$$Y_{+,n+1} = Y_{+,n}\left(\frac{h_{n+1}}{h_n}\right)^2\left(\frac{w_{+,n+1}}{w_{+,n}}\right)^2\left(\frac{Q_n}{Q_{n+1}}\right) \tag{5}$$

Using the Reynolds number definition and an orifice relation for supply flow, this becomes

$$Y_{+,n+1} = Y_{+,n}\left(\frac{R_{e,n+1}}{R_{e,n}}\right)\left(\frac{w_{+,n+1}}{w_{+,n}}\right)\left(\frac{P_{+,n}}{P_{+,n+1}}\right) \tag{6}$$

The input admittance of a given amplifier can be written in terms of its output admittance

$$Y_{i,n} = kY_{o,n} \tag{7}$$

where k is usually less than unity.

The admittance ratio $\left(\frac{Y_{o,n}}{Y_{o,n} + Y_{i,n+1}}\right)$ can now be written

$$\frac{Y_{o,n}}{Y_{o,n} + Y_{i,n+1}} = \frac{1}{1 + km^2\left(\frac{Re_{,n+1}}{R_e}\right)\left(\frac{P_{+,n}}{P_{+,n+1}}\right)\left(\frac{w_{+,n+1}}{w_{+,n}}\right)} \tag{8}$$

where

m = the number of parallel elements in the driven stage.

If elements are being staged for pressure gain, this admittance ratio is made to approach unity and m = 1. For maximum power gain, this ratio is set equal to 0.5 (for linear characteristics), and for flow gain, this ratio approaches zero and m > 1. From equations (3) and (8), for pressure gain (m = 1), the supply pressure ratio can now be defined as

$$\frac{P_{+,n+1}}{P_{+,n}} \equiv G_p - k(Re_r)(w_r) \tag{9}$$

where

$$Re_r \equiv \frac{Re_{,n+1}}{Re_{,n}} \quad \text{and} \quad w_r \equiv \frac{w_{+,n+1}}{w_{+,n}}$$

Consider now the design of a pressure gain stage. Assume that $G_p = 10$ and $k = 0.5$ (from measurements) and let

$$\frac{Re_{n+1}}{Re_{,n}} = \frac{w_{+,n+1}}{w_{+,n}} = 1 \ ;$$

then

$$P_{+,r} = \frac{P_{+,n+1}}{P_{+,n}} = 9.5$$

Then for constant Reynolds numbers, the height ratio $h_r (= h_{n+1}/h_n)$ is $1/\sqrt{9.5} = 0.3208$. Therefore, the proper staging has $P_{+,r} = 9.5$ and $h_r = 0.32$ for maximum dynamic range.

This may be too much of a change in depth between stages to be easily fabricated. If the Reynolds number range is sufficiently large, a Reynolds number ratio of 1.5 per stage can be used (i.e., 800, 1200, and 1800 for three stages). This increases $h_r$ from 0.3208 to 0.4812 or approximately one half. Higher Reynolds number ratios are not possible because of the limited range of Reynolds numbers for proper operation. The range is limited by jet stability at high Reynolds numbers and by low gain at lower Reynolds numbers.

The designer may need a power amplifier rather than a pressure gain block. For maximum power transfer, the admittance ratio, from data, $\left(\frac{Y_{o,n}}{Y_{o,n} + Y_{i,n+1}}\right) = 0.6$ is the maximum power point.

The supply pressure ratio $P_{+,r}$ is then $0.6G_p$, or 6 if the pressure gain per stage is 10. Since the next stage will have a higher supply pressure, the output must be used to drive multiple succeeding stages to achieve maximum power transfer. From equation (8), m, the number of parallel units in the driven stage, can be defined as

$$m^2 = \frac{0.667 P_{+,r}}{k Re_r w_{+,r}} \tag{10}$$

since the admittance ratio 0.6. For $k = 1$, $Re_r = 1$, $w_{+,r} = 1$, $P_{+,r} = 6$, the number (m) of parallel units in the driven stage is 2 ($m = 2$). In summary,

$$P_{+,r} = 6; \quad m = 2; \quad h = \frac{1}{\sqrt{6}} = 0.4$$

for maximum power gain.

For maximum flow gain, defined as flow gain when pressure gain is unity, $P_{+,r} = 1$ and the admittance ratio

$$\frac{Y_{o,n}}{Y_{o,n} + Y_{i,n+1}} = \frac{1}{G_p}$$

so that

$$m^2 = \frac{G_p - 1}{k Re_r w_{+,r}} \tag{11}$$

If $G_p = 10$, $k = Re_r = w_{+,r} = 1$, then $m = 3$ for maximum flow gain. These three approaches are summarized in figure 10. For pressure gain alone (flow gain unity), $m = 1$ and $P_{+,r}$ is determined essentially by blocked output pressure gain. For maximum power gain, the admittance ratio is set equal to 0.6 (maximum power point on output characteristic). This sets the supply pressure ratio at 0.6 times the blocked output pressure gain. Using this, m is determined from the admittance ratio definition. For maximum flow gain (pressure gain equal to unity), the admittance ratio is set equal to the reciprocal of the blocked area pressure gain, and then m (the number of parallel elements in the driven stage) is determined from the definition of the admittance ratio (eq 8).

## 5. DESIGN

In figure 3, the laminar jet amplifier is shown. This design incorporates two changes of the model of Griffin and Gebben.[2] First, to reduce the output admittance, no center dump is used; second, the distance between downstream edges of the control nozzles was reduced from $2.5w_+$ to $2.0w_+$. The element of figure 3 has the following normalized parameters:

Control nozzle = $4w_+$ measured along the jet boundary

Distance to splitter
from supply nozzle exit = $8w_+$

Receiver width = $1.5w_+$

The importance of these dimensions will be discussed in the analysis section.

The element in figure 3 was fabricated in 0.25-mm, 0.50-mm, and 1.0-mm depths. Each element was individually tested and provided a

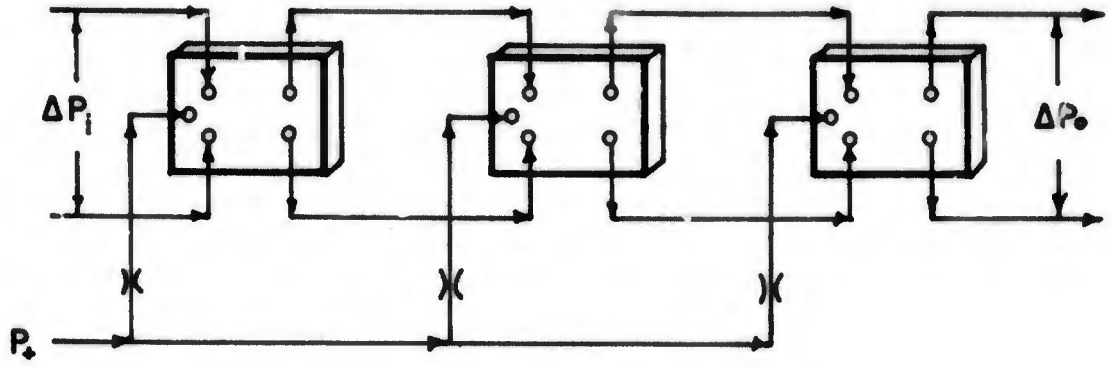


(a) PRESSURE GAIN

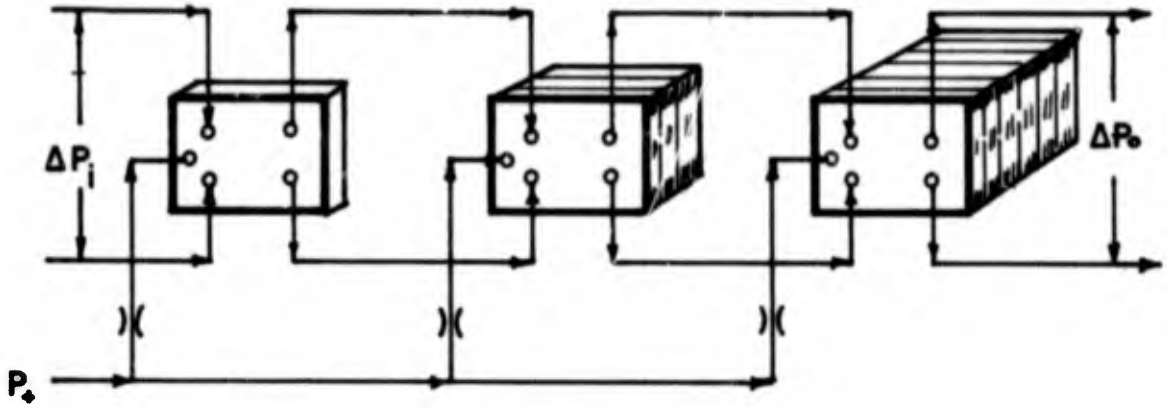


(b) FLOW AND/OR POWER GAIN

Figure 10. Staging method.

blocked output area pressure gain of about 14. Figure 11 shows the pressure gain characteristic of a three-stage pressure gain block. The pressure gain is about 1000 and the saturation characteristic does not reverse. But there is a null shift in the gain curve. This is probably caused by mechanical bias in the elements. Figure 12 shows the interconnection operating points for stages 1 and 2, and for stages 2 and 3. The actual staging efficiency (ratio of staged pressure gain to blocked output area pressure gain is 0.75 for both couplings between stages. This efficiency is lower than expected, probably because of line loss in the tubing used for interstage coupling.

The staging efficiency was shown (sec. 4) to be calculated by the ratio of output admittance to total admittance. Using the Reynolds number ratio, the supply pressure ratio, and the input-to-output admittance ratio, the staging efficiency can be calculated.

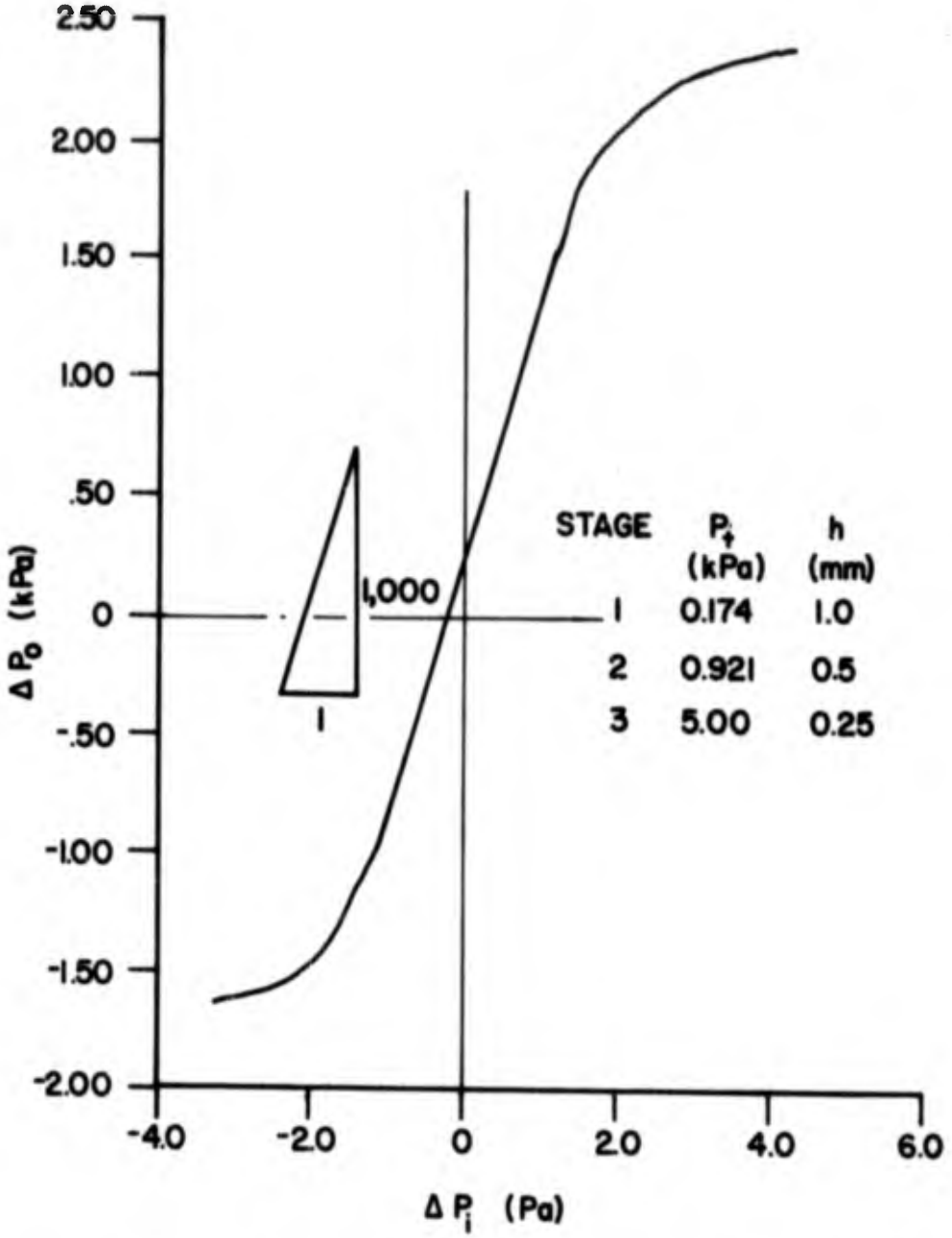


Figure 11. Pressure gain of a three-stage gain block.

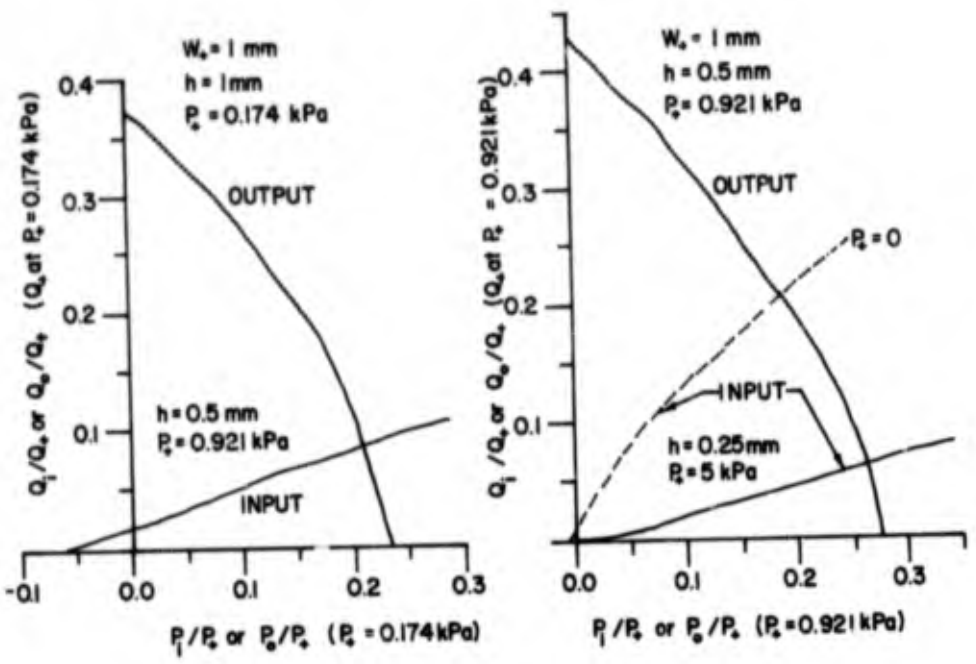


Figure 12. Input and output characteristic of the gain block.

$$\text{Staging Efficiency} = \frac{\text{staged gain}}{\text{blocked output gain}} = \frac{Y_o}{Y_o + Y_1} \qquad (12)$$

$$= \frac{1}{1 + kRe_r/P_{+,r}}$$

for identical plan view devices. In figure 12b, the input and output characteristics of a model element for the 0.5-mm depth is shown. The scales are normalized to the supply pressure and flow of this element. The input characteristic of the 0.25-mm driven stage (same model) is superimposed on this figure. We have k = 0.63 (i.e., the element's input-output admittance ratio) in figure 5; the output characteristic intersects this element's input characteristic at 63% of the blocked output area pressure; the $P_+$ ratio of 1/0.185 and a Reynolds number ratio of 1.162 were used in the test. Combining these, the staging efficiency is

$$\text{Staging Efficiency} = \frac{1}{1 + (0.63)(1.162)(0.185)} = 0.88 \qquad (13)$$

However, this is not quite accurate because k is not constant. If a polynomial of the form $\bar{Q}_o = a + b\bar{P}_o + c\bar{P}_o$ is fitted to the normalized output data of figure 12b, the best fit is ($\bar{Q}_o = 0.409 - 0.580\bar{P}_o - 2.182\bar{P}_o^2$) and

$$\left.\frac{\partial \bar{Q}_o}{\partial \bar{P}_o}\right|_{\frac{\bar{P}_o}{\bar{P}_{o,max}} = 0.9}^{\bar{P}_o = 2.0}$$

$\frac{\bar{P}_o}{\bar{P}_{o,max}}$ is set at 0.9 since this is close to the actual operating point. From these numbers, k = 0.5 and the staging efficiency is 0.9. This is in good agreement with operating point data of figures 12a and 12b and shows that the driven stage has higher input impedance than the output impedance of the driving stage. Therefore, high multi-stage pressure gains can be obtained.

For an element depth ratio of 0.5 and a Reynolds number ratio of 1.5, the supply pressure ratio from stage to stage should be 9.36. The data of figure 12 was taken for supply pressure ratio $P_{+_1 r} = 5.4$ and a Reynolds number ratio of 1.1625. These were experimentally obtained before the correct staging of these elements was determined. The pressure losses in interstage lines reduce the supply pressure ratio and they were not included in the staging estimate. However, these losses should be minimal in an integrated package. In the early experiments, staging for pressure gain was the goal since it is easily measured. The Reynolds number ratio from stage to stage was 1.1625 rather than the desired 1.5. For a given depth ratio, a decrease in Reynolds number ratio reduces the dynamic range. The dynamic range is apparently reduced by 1.75 per stage (9.36/5.4) or 3.06 for the staged assembly. Individual stage dynamic range is about 1200. Multistage dynamic range appears to be about 400, which is the ratio of 3. More work is needed to properly stage these elements.

No experimental work has yet been performed on maximum power gain staging or maximum flow gain staging, since the element is still being refined and the necessary depths are not yet available.

## 6. ANALYSIS

The purpose of this analysis is to describe the dependence of element pressure gain, control bias sensitivity, and frequency response on the geometrical structure, Reynolds number, and supply pressure. The analysis is linear for estimates of small signal response around the null.

This analysis describes the laminar proportional amplifier shown in figure 3 by means of the control volume method. Figure 13 shows the control volume set that was considered. The vents are assumed to have zero resistance so that this description concentrates on the jet deflection due to the pressure in only one set of control volumes.

The sum of flows in one of the control volumes is given by

$$Y_i(P_i - P_1) - Q_e - Y_1 P_1 = Y_c P_i \qquad (14)$$

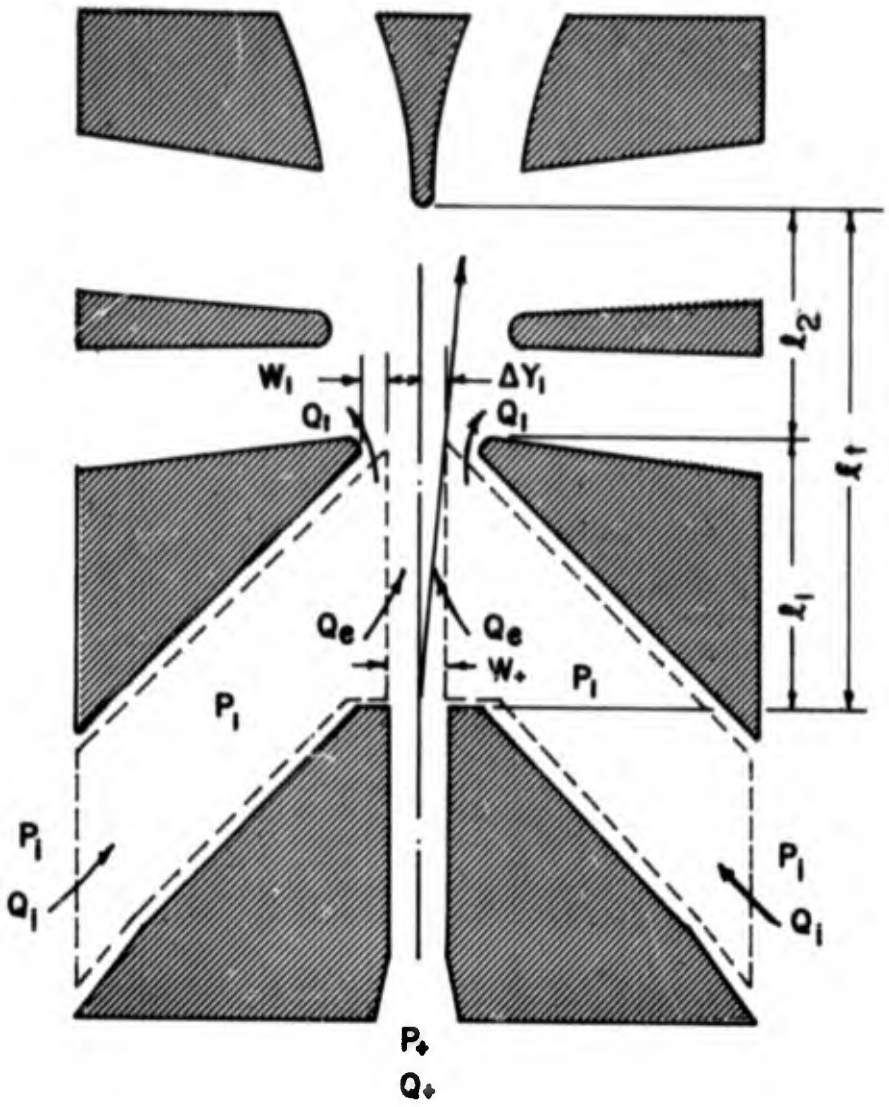


Figure 13. Control volume used in analysis.

where

$Y_i(P_i - P_1)$ = input flow on one side ($m^3/s$)

$Y_1P_1$ = control volume outflow ($m^3/s$)

$Y_i$ = input admittance [$m^3/(kPa-s)$]

$Y_1$ = control volume output admittance [$m^3/(kPa-s)$]

$Y_c$ = capacitive admittance of jet configuration [$m^3/(kPa-s)$]

$P_i$ = input pressure (kPa)

$P_1$ = control volume static pressure (kPa)

$Q_e$ = entrained flow ($m^3/s$)

An important point to note is that the control volume output admittance is modulated by the lateral displacement of the jet at the end of the control nozzle. This output admittance is of the orifice type, therefore the area modulation effect can be written as

$$Y_1 = Y_{10}\left(1 \pm \frac{\Delta y_1}{w_1}\right)^2 \tag{15}$$

where

$Y_{10}$ = control volume output admittance for $\Delta y_1 = 0$

$w_1$ = the outlet width defined by jet boundary and downstream edge of the control nozzle structure

$\Delta y_1$ = the jet displacement at the downstream edge of the control nozzle

For convenience, the admittances are normalized by the supply operating point admittance $Y_+$, which is the supply flow divided by the supply pressure. Normalizing, we have

$$\bar{Y}_{10} = \frac{Y_{10}}{Y_+} = \left(\frac{Q_1}{Q_+}\right)\left(\frac{P_+}{P_1}\right) \tag{16}$$

Since

$$P_+ = \frac{\rho}{2}\left(\frac{Q_+^2}{w_+^2 h^2}\right) \quad ; \quad P_1 = \frac{\rho}{2}\left(\frac{Q_1^2}{w_1^2 h^2}\right)$$

we have

$$\bar{Y}_{10} = \left(\frac{w_1}{w_+}\right)^2 \left(\frac{Q_+}{Q_1}\right) \tag{17}$$

where

$h$ = the depth of the unit

$w_+$ = the supply nozzle exit width

$\rho$ = the fluid density which is assumed constant

The jet's deflection depends on the difference in pressure between the two control volumes, since the control momentum flux is negligible in this model. Taking the difference of the flows between volumes using equations (14) and (15) results in the difference equation

$$\bar{Y}_1(\Delta P_1 - \Delta P_1) - 2\bar{Y}_{10}\left(\frac{\Delta y_1}{w_1}\right)(P_{11} + P_{12}) - \bar{Y}_{10}\left[1 + \left(\frac{\Delta y_1}{w_1}\right)^2\right]\Delta P_1 = \bar{Y}_c \Delta P_1 \tag{18}$$

where

$\bar{Y}_c$ = compliance admittance of jet

$P_{11}$ = control volume pressure on side 1

$P_{12}$ = control volume pressure on side 2

and the admittances are normalized with respect to $Y_+$. This assumes that the difference in entrained flow is negligible. The non-linear output admittance results in a sum term as well as a difference term in control pressure.

Defining

$$Y_T = Y_i + Y_{10}\left[1 + \left(\frac{\Delta y_1}{w_1}\right)^2\right] + Y_c$$

then from equation (18),

$$\Delta\bar{P}_1 = \frac{Y_i}{Y_T}\ \Delta\bar{P}_i - 2\left(\frac{Y_{10}}{w_1}\right)\left(\frac{\Delta y_1}{w_1}\right)(\bar{P}_{11} + \bar{P}_{12}) \tag{19}$$

The jet is deflected by the difference in control volume pressure along distance $\ell_1$ (fig. 13), the effective length of the control volume; then it continues in the direction it has attained at the end of the control volume, as shown by the deflected jet centerline in figure 13.

The angle the jet makes with the amplifier axis at the end of the control volume is

$$\theta = \frac{\bar{\ell}_1 \Delta\bar{P}_1}{2} \tag{20}$$

The lateral displacement of the jet at the end of the control volume for a constant pressure difference is

$$\Delta\bar{y}_1 = \frac{\bar{\ell}_1^{\,2}}{4}\Delta\bar{P}_1 \tag{21}$$

($\Delta\bar{P}_1$ is normalized with respect to $P_+$; $\Delta\bar{y}_1$ and the effective length of the control volume, $\bar{\ell}_1$, are normalized with respect to $w_+$.) Substituting equations (21) into (19) and eliminating $\bar{y}_1$, one obtains

$$\Delta\bar{P}_1 = \frac{Y_i}{Y_+}\,\Delta P_i\left[\frac{1}{1 + 2\frac{Y_{10}}{Y_+}\left(\frac{1}{w_1}\right)\left(\frac{\ell_1}{4}\right)(\bar{P}_{11} + \bar{P}_{12})}\right] \tag{22a}$$

If

$$\bar{P}_{11} + \bar{P}_{12} = 2\bar{P}_1$$

assuming a push-pull control pressure signal, then $\Delta\bar{P}_1$ can be written as

$$\Delta\bar{P}_1 = \frac{\left(\frac{Y_i}{Y_T}\right)\Delta\bar{P}_i}{1 + \left(\frac{\ell_1}{w_1}\right)\left(\frac{Y_{10}}{Y_T}\right)(\bar{P}_1)} \tag{22b}$$

(This bias level of $\bar{P}_1$ determines the pressure difference, $\Delta\bar{P}_1$, from an input signal, $\Delta\bar{P}_1$.)

The total jet deflection, $\Delta y_T$, at the receiver entrance plane is

$$\Delta\bar{y}_T = \Delta\bar{y}_1 + \bar{\ell}_2\theta \tag{23}$$

where

$\ell_2$ = downstream spacing between the control nozzle and the receiver (fig. 13)

Using equations (20) and (21) with equation (23)

$$\Delta\bar{y}_T = \Delta\bar{P}_1 \frac{\bar{\ell}_1^2}{4} + \frac{\bar{\ell}_1\bar{\ell}_2}{2} \tag{24}$$

Define $\bar{\ell}_T = \bar{\ell}_1 + \bar{\ell}_2$ as the total separation between the power jet nozzle exit and the receiver. By using $\bar{\ell}_T$, $\Delta\bar{y}_T$ is

$$\Delta y_T = \frac{\bar{\ell}_1^2}{4}\left(\frac{2\bar{\ell}_T}{\ell_1} - 1\right)\Delta\bar{P}_1 \tag{25}$$

Dropping the bars and using equation (22b), the total jet displacement at the entrance to the receiver is then

$$\Delta y_T = \frac{\left(\frac{\ell_1^2}{4}\right)\left(\frac{2\ell_T}{\ell_1} - 1\right)\left(\frac{Y_i}{Y_T}\right)\Delta P_1}{1 + \left(\frac{\ell_1^2}{w_1}\right)\left(\frac{Y_{10}}{Y_T}\right)P_1} \tag{26}$$

The difference in jet pressure available at the receiver entrance, $\Delta P_o$, is found by multiplying $\Delta y_T$ by the quotient $\Delta P_o/\Delta y_T$. By estimating this quotient from experimental data on many receiver configurations, the pressure gain is obtained as follows:

$$\text{Pressure Gain} = \frac{\Delta P_o}{\Delta P_i} = \left(\frac{\Delta P_o}{\Delta y_T}\right)\frac{\left(\frac{\ell_1^2}{4}\right)\left(\frac{2\ell_T}{\ell_1} - 1\right)\left(\frac{Y_i}{Y_T}\right)}{1 + K_1 P_1} \tag{27}$$

where

$K_1 = \frac{\ell_1^2}{w_1}\left(\frac{Y_{10}}{Y_T}\right)$ , the bias coefficient.

If $\Delta P_o/\Delta y_T$ is taken as 1.0, $\ell_1 = 4$ (i.e., $4w_+$), $\ell_T = 8$ (i.e., $8w_+$), and from input measurements of an early model amplifier, $Y_i/Y_T$ for zero frequency is 0.7 and $Y_{10}/Y_T = 0.3$; since measurement of the pressure and flow out of the control volume indicate $w_1 = 0.20$ ($0.20w_+$), the pressure gain is estimated to be

$$\frac{\Delta P_o}{\Delta P_i} = \frac{7.56}{1 + 24P_1} \tag{28}$$

In general, it is easier to measure $P_i$ rather than $P_1$; therefore an expression for $P_1$ in terms of $P_i$ is substituted in this equation.

$$P_1 - P_{1o} = (P_i - P_{io})\frac{Y_i}{Y_T} \tag{29}$$

This equation is obtained from experimental data and is shown schematically in figure 14. The negative pressure, where $P_i = P_1$, is for a sealed inlet and is due to jet entrainment, and is defined as $P_{io}$. Substituting this expression for $P_1$ into equation (27), the pressure gain can be expressed as a function of the inlet pressure level in equation (29); therefore, for $\omega = o$ we have

$$\frac{\Delta P_o}{\Delta P_i} = \left[\frac{\Delta P_o}{\Delta y_T}\right] \frac{\dfrac{\left(\frac{\ell_1}{4}\right)^2\left(\frac{2\ell_T}{\ell_1} - 1\right)\left(\frac{Y_i}{Y_T}\right)}{1 + \left(\frac{\ell_1^2}{w_1}\right)\left(\frac{Y_{10}}{Y_T}\right)^2 P_{io}}}{1 + \dfrac{P_1\left(\frac{\ell_1}{w_1}\right)^2\left(\frac{Y_{10}}{Y_T}\right)\left(\frac{Y_i}{Y_T}\right)}{1 + \frac{\ell_1^2}{w_1}\left(\frac{Y_{10}}{Y_T}\right)^2 P_{io}}} \tag{30a}$$

or

$$\frac{\Delta P_o}{\Delta P_i} = \frac{8.83}{1 + 19.6P_i} \tag{30b}$$

where

$P_{io}$ = the inlet pressure when the inlet is sealed; for our measurements, it was $-0.02P_+$.

Equation (30b) is in good agreement with unpublished data by Hellbaum [of NASA (Langley)] that gives pressure gain as a function of $P_i$, not $P_1$, as shown in figure 15. Therefore, equations (30) are good descritpions of the sensitivity of the amplifier's pressure gain figure to bias, for small input signals.

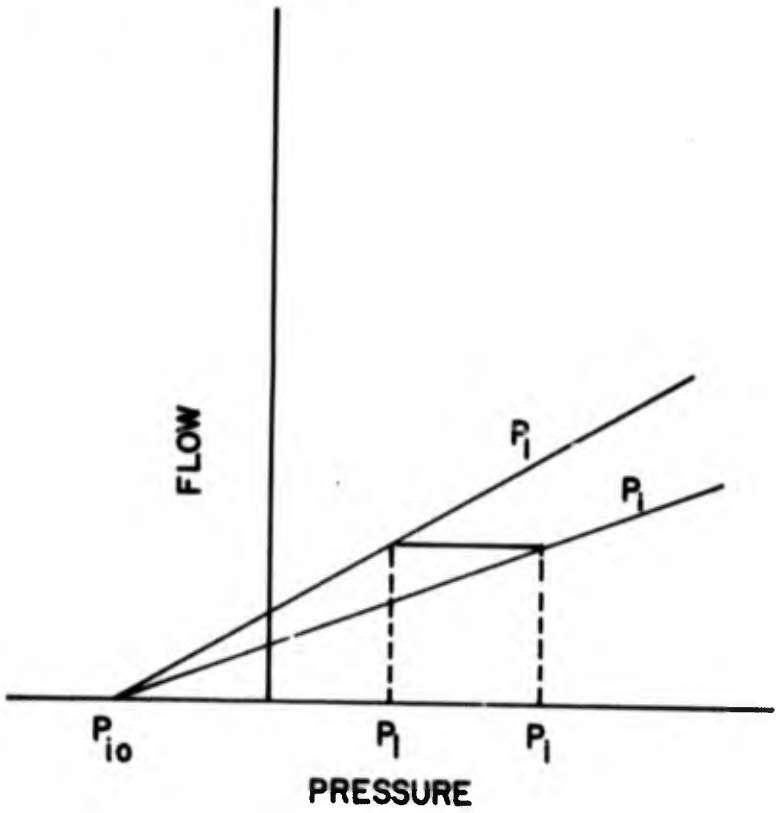


Figure 14. Input characteristic.

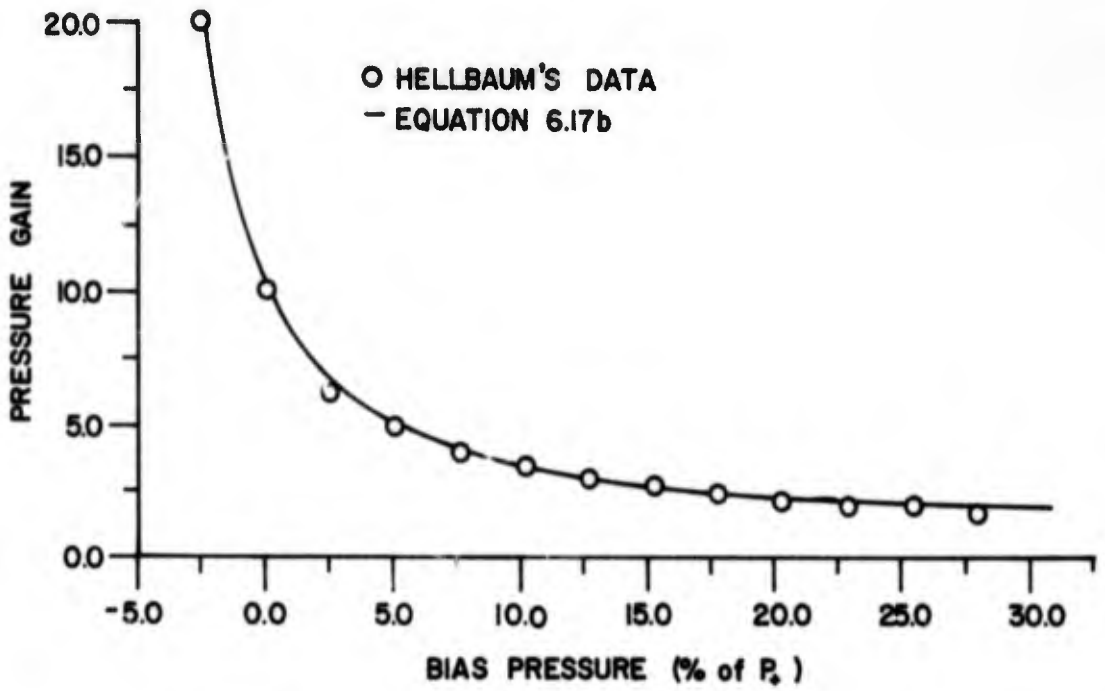


Figure 15. Effect of bias pressure on pressure gain.

6.1 Amplifier Gain

The pressure gain given by equation (27) for a zero bias pressure ($P_1$) level is

$$G_p = \frac{\Delta P_o}{\Delta y_T} \left(\frac{\ell_1^2}{4}\right)\left(\frac{2\ell_T}{\ell_1} - 1\right) \frac{Y_i}{Y_T} \qquad (31a)$$

For the amplifier of figure 3, $\ell_1 = 4$, $\ell_T = 8$, and $Y_i/Y_T = 0.9$. Substituting these values into equation (31a), the pressure gain is calcualted to be

$$G_p = \left(\frac{\Delta P_o}{\Delta y_T}\right) (10.8) \qquad (31b)$$

The measured pressure gain, however, is about 14 to 18. If our scale factor is correct, this implies that $P_o/ y_T > 1$, which is unlikely. If we have a two-dimensional jet at the receiver, this coefficient would be about one. It is more reasonable to suppose that the jet is deflected more by the control pressure than our scale factor indicates. The jet deflection must be 1.7 times that predicted. This increased deflection results because the momentum flux from the supply jet is actually less than that calculated on the basis of the pressure difference across the power supply nozzle.

Drzewiecki (of HDL) has used the Karman-Pohlhausen integral method to calculate the boundary layer thickness for the supply nozzle used in this amplifier. (His analysis for discharge coefficient shows very good agreement with experiment.) His results showed a discharge coefficient of 0.587 for this element which agrees with experiment. If this method is applied to the momentum flux, a momentum flux discharge coefficient of 0.452 is calculated. Therefore, the supply momentum flux is reduced to 45.2% of that associated with a perfectly square profile, and consequently the scale factor must be multiplied by 1/0.452 or 2.213. Therefore equation (31b) becomes

$$G_p = \left(\frac{\Delta P_o}{\Delta y_T}\right) (23.9) \qquad (31c)$$

The decreased momentum means that the jet is softer and bends further than expected for a given control signal. If the jet does not spread too much, the output pressure gain (blocked output area) can increase, but the element has a lower output admittance. This results from the rather developed velocity profile at the receiver entrance. Also, the jet compliance is increased because there is more displacement for a given control signal. At lower Reynolds numbers, the reduction in available output is caused by jet spread so that receiver characteristics or the scaling coefficients need to be revised to include this effect. However, if we limit the Reynolds number range (as discussed in sec. 2), this complication can be avoided.

Since laminar jet analysis (two-dimensional) shows that $\Delta P_o/\Delta y_T$ can approach unity, then pressure gains of up to 23.9 can be expected. Blocked output pressure gains of about 24 have been obtained in the laboratory; however, gains of 14-18 are normally measured when care has been taken to assure that the control bias level is zero and not negative. This means $\Delta P_o/\Delta y_T \approx 0.75$.

### 6.2 Control Bias Sensitivity

The bias sensitivity is dependent on the area modulation of the control. This sensitivity is determined by the bias coefficient $K_1$ or $K_i$, depending on the definition of bias level [i.e., the $P_1$ or $P_i$ coefficient in the numerator of equation (27) or (30a)]. If the average control bias level is positive, these coefficients reduce the pressure gain. If the bias level is negative, the gain is increased, which can account for some of the high gain measurements. Typically, the output of the driving stage sets the bias level for the driven stage, and $K_1$ or $K_i$ must be reduced to maintain the pressure gain $G_{po}$. If $R_1$ is an orifice type resistance, then a reduction of $w_1$, the width of the orifice spacing of the downstream control nozzle structure from $2.5w_+$ to $2.0w_+$, would reduce $K_1$ from 33 to 12.7. These numbers are of course approximate and depend on the input operating point. With a reduced $K_1$, amplifiers have been successfully staged without a significant gain reduction.

A commercial amplifier was tested and found to have about 1 percent of the bias sensitivity of the element shown in figure 2. This is attributed to the reduction of the control nozzle width squared ($\ell_1^2$) from 16 to 2.25 and the reduction of the outlet spacing between the jet and the edge of the control nozzle, which determines the control volume outlet orifice, from 0.75 to $0.25w_+$. This means their $w_1$ was very small; therefore, it is not surprising that the value of $K_1$ is very small. In our study, $w_1$ has not been reduced further to

allow a full deflection of the jet. A gain-maximum deflection product should be considered in selecting a proper spacing for $w_1$.

Griffin and Gebben[2] fit the pressure gain-pressure bias data curve with a $K_1$ of 8.35. Their $K_1$ is small because their jet was turbulent and therefore it spread more, reducing the effective spacing between the downstream control structure and the jet boundary.

This approach to reduce bias sensitivity by reducing $w_1$ depends on the flow through $w_1$ exhibiting an orifice characteristic, so that a decrease in $w_1$ decreases $Y_1$ more than it increases $1/w_1$. If this outflow has a linear (laminar resistor) characteristic, then the magnitude of $K_1$ or $K_i$ is not changed by reducing $w_1$. The bias sensitivity effect can be reduced for this case by using a large supply pressure ratio since the bias pressure is normalized with respect to that stage's supply pressure.

### 6.3 Estimate of Dynamic Response

The dynamic response of this amplifier appears to be limited by the dynamics associated with the deflecting control pressure field. Receiver dynamics, vent dynamics, and all the various couplings must be carefully considered in evaluating an amplifier's dynamic range. This section will only be concerned with the dynamics of the inlet and control deflecting field. This limitation is justifiable because the jet compliance is large for the very low pressure jet stream used in the first stage. The first stage for constant size (plan view) elements limits the response of the three-stage gain block. Our experimental results for this stage indicate that receiver and vent dynamics play a secondary role. To estimate the dynamic response of the control field, the control volume analysis is used.

The control volume analysis is valid for small signals with symmetrical inputs around a given level. The flow is assumed to be incompressible and laminar. Symmetry allows one to analyze only one control volume, rather than the difference set, to estimate the dynamics of the jet deflecting field. The control volume analysis shows that the jet deflection pressure is the admittance ratio $Y_i/Y_T$ times the input pressure signal. $Y_i/Y_T$ is a simple RLC T-network, but the dynamics are made more complex by a non-zero control bias level. The ratio of dynamic pressure gain to zero-frequency pressure gain is given by

$$\frac{G_p}{G_{p|\omega=0}} = \frac{\left(\frac{L_1}{R_L}s + 1\right)}{\left(\frac{L_1L_1C}{R_i' + R_1}\right)s^3 + \left(\frac{L_1R_i + L_iR_1}{R_i' + R_1}\right)Cs^2 + \left(\frac{R_1R_iC + L_i' + L_o}{R_i' + R_1}\right)s + 1} \qquad (32)$$

where

$$R_i' = R_i\left(1 + \frac{\ell_1^2}{w_1}P_1\right)\left[1 + \left(\frac{\Delta y_1}{w_i}\right)^2\right]$$

$$L_i' = L_i\left(1 + \frac{\ell_1^2}{w_1}P_1\right)\left[1 + \left(\frac{\Delta y_1}{w_i}\right)^2\right]$$

$P_1$ = bias control pressure

$\ell_1$ = control nozzle width

$w_1$ = effective outlet width

s = Laplace operator

$\omega$ = frequency

L = inductance (inertance)

R = resistance

C = jet capacitance (compliance)

In analyzing the control volume network, it is helpful to normalize the parameters by the supply pressure, the supply flow, and the supply resistance ($P_+/Q_+$ at the operating point). In scaling the equations, time is normalized by dividing by $w_+/V_+$ defined as $t_+$--one nozzle width transport time. When the network parameters are so normalized they become

$$\overline{L} = 2\ell/w \quad : \quad \ell \text{ is inductive channel length and w is the channel width}$$

$$\overline{C} = \overline{\ell}_1 \forall 6 \quad : \quad \overline{\ell}_1 = \ell_1/w_+, \text{ the control nozzle length along the jet}$$

$$\overline{R} = R/R_+ = RQ_+/P_+ \tag{33}$$

and

$$\overline{t} = t/t_+$$

The values used for these parameters in the calculation were

$$\begin{array}{lll} \overline{L}_1 = 10 & \overline{C} = 23.45 & \overline{R}_1 = 0.9 \\ \overline{L}_1 = 4 & (\overline{C} = 10.66/0.452 \text{ where } 0.452 \text{ is normalized momentum flux of jet stream.}) & \overline{R}_1 = 0.1 \end{array} \tag{34}$$

The frequency response for these parameters is shown in figure 16. The time scaling parameter, $t_+ = w_+/V_+$, is used so that the frequency is scaled by $V_+/w_+$. The average supply jet velocity, $V_+/w_+$, is the Bernoulli dynamic velocity multiplied by the discharge coefficient. The effects of (slightly positive and slightly negative) bias pressure are shown. The positive bias level increases the damping, and a negative bias decreases the damping. The frequency response of all elements of this same plan view operating in the laminar regime can be estimated using this figure within the accuracy of the circuit parameters and the validity of the assumptions [i.e., no receiver (or vent) effects]. In equation (15), the outlet admittance $Y_1$ is defined as $Y_{10}[1 + (\Delta y/\omega_1)^2]$. For small signal analysis, $\Delta y^2 << w_1$ and the effect of area modulation is limited to the cross product term that results in the bias sensitivity of the amplifier. However, if the amplifier is overdriven or driven by signals large enough to cause $\Delta y/w_1 = 1$ then $Y_1 = 2Y_{10}$. The effect of this is to increase the damping in the

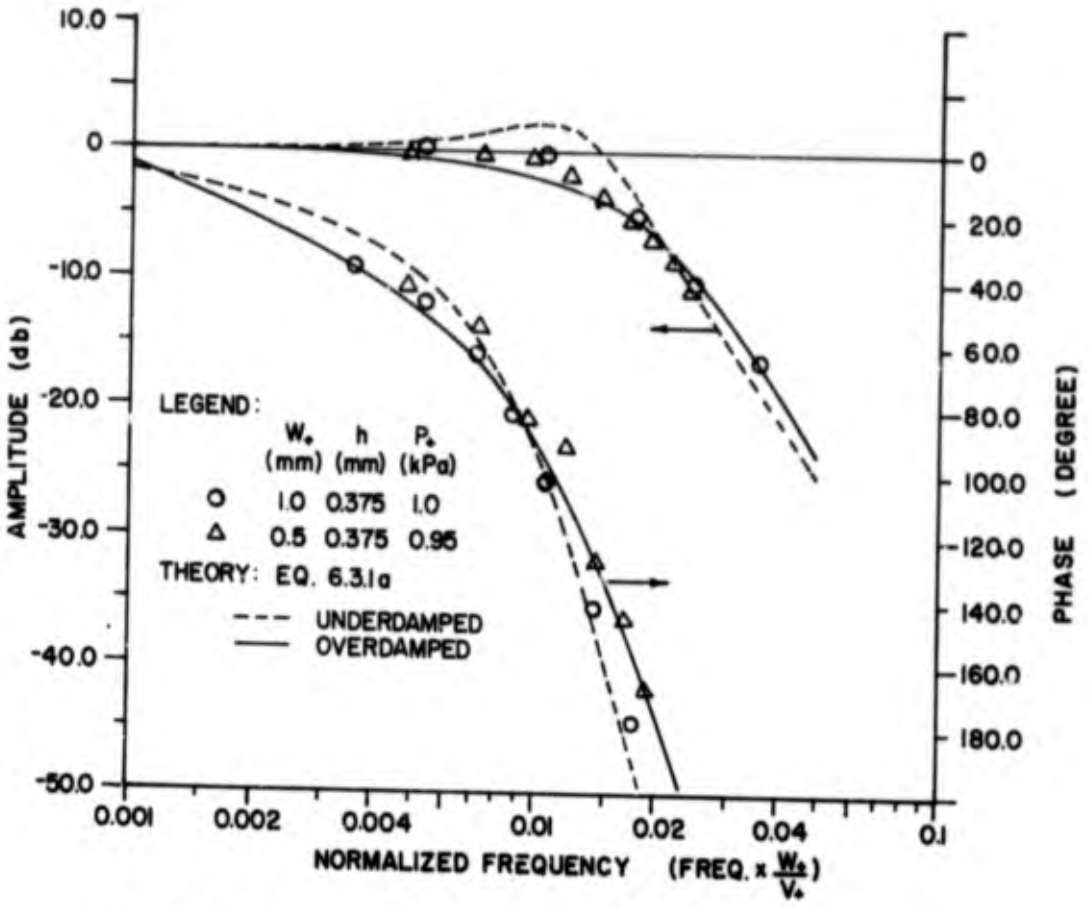


Figure 16. Frequency response of laminar proportional amplifier.

element's frequency response. This is interesting since when the input signal is large for zero frequency, the device has a saturation output signal. But if it is driven by a large sinusoidal input signal, the output signal is overdamped. These characteristics are desirable in control system applications. The effect of overdriving the amplifier is the same as operating with a positive bias level, i.e., overdamped response as shown in figure 16.

Figure 17 shows the amplitude response of the amplifiers (fig. 3) using the swept frequency dynamic response apparatus described by Toda, Roffman, and Talkin.[3] Data from elements with $w_+$ = 1 mm, h = 0.25 mm, and $w_+$ = 0.5 mm, h = 0.375 mm are shown. The 1- by 0.25-mm element operated at a supply pressure of 5 kPa and has a slightly underdamped response of 600 to 700 Hz. The 0.5- by 0.375-mm element operated at a supply of 0.95 kPa, has a dynamic response of 465 Hz, and is overdamped.

---

[3] Toda, K., Roffman, G.L., and Talkin, A.I., "Fluerics 30. The Matched Acoustic Generator," HDL-TR-1574, December 1971, Harry Diamond Laboratories, Washington, D.C. 20438.

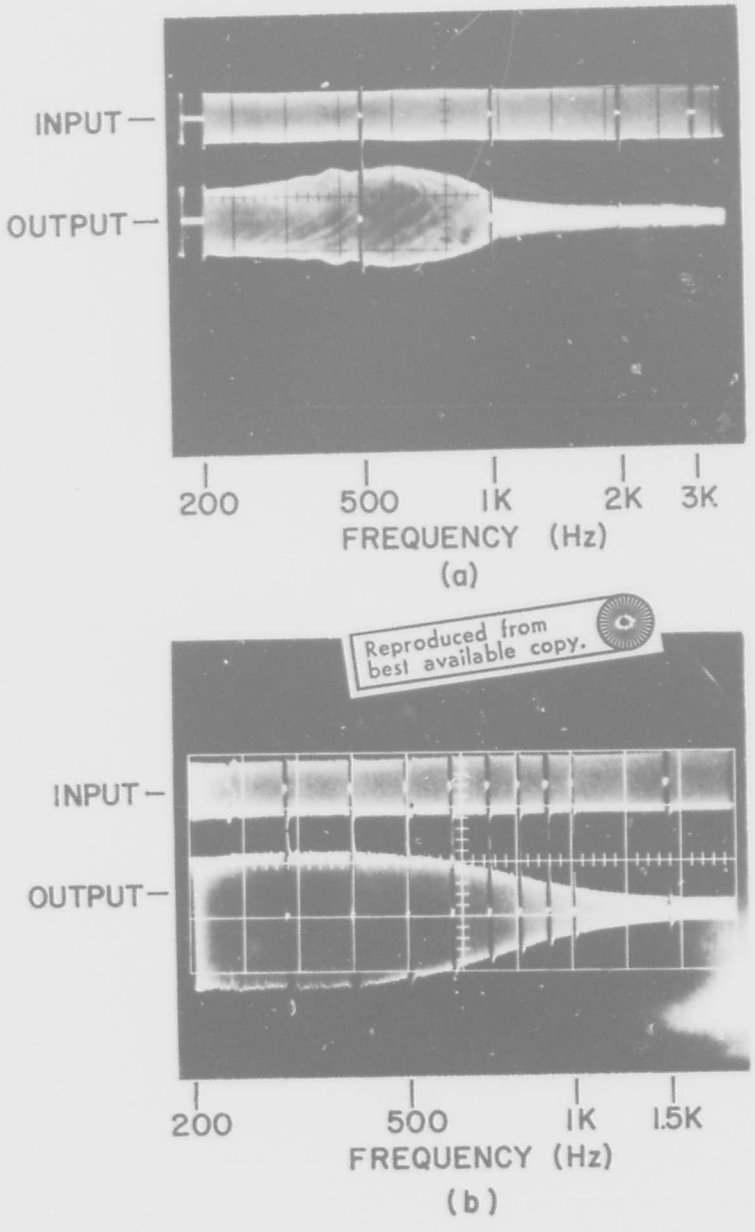


Figure 17. Amplitude response of laminar proportional amplifier.

The discharge coefficient was calculated in each case and good agreement was obtained with experimental data. For example, at $P_+ = 5$ kPa, the average supply velocity is $V_{+,av} = 50.4$ m/sec since the discharge coefficient is 0.56. Therefore, for a nozzle width $w_+ = 1.0$ mm, $V_{+,av}/w_+ = 50{,}400$. The cutoff frequency (fig.16) occurs in the vicinity of 0.011 to 0.012 times $V_+/w_+$. For $V_{+,av}/w_+ = 50{,}400$, this yields a frequency between 550 and 600 Hz. For $w_+ = 0.5$ mm, $h = 0.375$ mm, and $P_+ = 0.95$ kPa, the discharge coefficient is 0.59. For that case, we have $V_{+,av}/w_+ = 46{,}880$ and therefore the cutoff frequency is 515 to 561 Hz. However, this element had high gain and it was almost impossible to operate with truly small signals and control the input amplitude. As a result, this element was overdriven and its response appears overdamped. To demostrate scaling in frequency in figure 16, the amplitude and phase data are shown of the 0.5 mm × 0.375 mm element and of the 1 mm × 0.375 mm element that operates at $P_+ = 1$ kPa. The latter element has a roll-off frequency of 280 Hz because it operates at a higher supply pressure and has a higher discharge coefficient.

The agreement obtained indicates that the models can be scaled. Other preliminary data taken for a 1 mm × 1 mm model ($P_+ = 0.25$ kPa) has approximately the calculated bandwidth. These results justify the assumption that neglected the influence of the vent and receiver dynamics. However, it is still worthwhile to estimate the vent and receiver response.

Using normalized parameters and noting that the jet momentum flux is 0.452 of a perfectly uniform profile,

$$\bar{C}_{jv} = \frac{\ell_v}{6} \times \frac{1}{0.452} \simeq 3$$

$$\bar{L}_v \simeq \frac{2\ell_v}{w_v} = 4$$

neglecting damping

$$\overline{LC}_v = 12 \text{ and } \frac{1}{2\pi\sqrt{LC}} = 0.0459 \times \frac{V_{+,av}}{w_+}$$

This is a factor of 4.6 times the input response which is shown in figure 16 as $0.01V_{+,av}/w_+$.

The receiver response can be estimated in a like manner, for a $5w_+ \times 5w_+ \times w_+$ volume.

$$C = \frac{\text{Volume}}{\gamma \bar{P}_{amb}} = \frac{25}{25\gamma} = 0.7$$

where

$$\bar{P}_{amb} = \frac{P_{ambient}}{P_+} = 25$$

$\gamma$ = ratio of specific heats

$$L = \frac{2\ell_r}{w_r} = 8$$

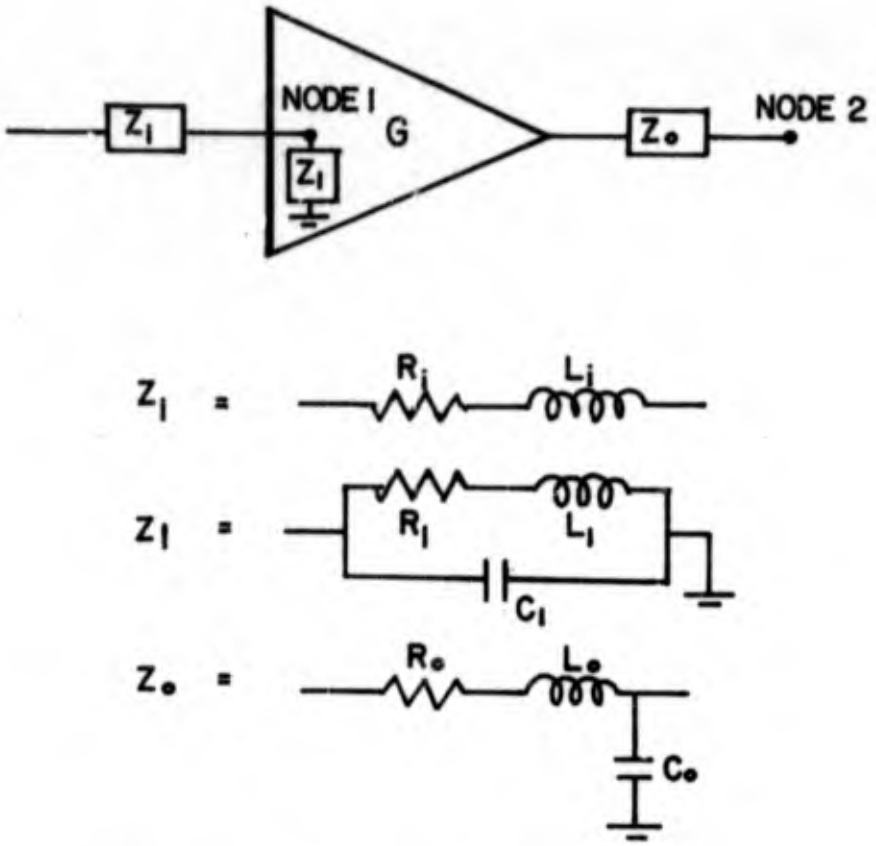


Figure 18. Schematic of the integrated gain block.

LC is therefore about 5.6 and consequently the resonant frequency is 0.067. This gives a factor that is 6.7 times greater than our calculated normalized frequency of 0.01. These frequencies are sufficiently greater than the "scaled" 0.01 Hz to justify the assumptions neglecting them. Attached as table I is a calculated amplitude and phase for an equivalent circuit shown in figure 18. The calculated response of figure 16 is for node 1 in this table listing. The output response is for node 2. The data listing shows that the influence of the receiver is small and does not influence the response until the amplitude is greatly attenuated. However, if a larger volume were used as an output port, or if the supply pressure were higher, the receiver response could not be neglected.

In multistage designs where the supply pressure is increasing from stage to stage, the dynamic response is limited by the first stage (low pressure stage). For example, if $P_{+_{r}} = 5$, then the second stage average velocity $V_+ = \sqrt{5} \times V_+$ of the first stage, and the third stage $V_+$ is 5 times the first stage. In table II, the gain and phase shift for three amplifiers of figure 18 connected in cascade are calculated. The inductance (inertance), capacitance, and resistance were calculated and were scaled by the square root of the $P_+$ ratio, i.e., $P_{+2}/P_{+1}$ and $P_{+3}/P_{+1}$. These were 5 and 25, respectively. These results indicate the response is determined by the first stage element for the values given. We plan to confirm these results by experiment.

TABLE I

Bode Plot Data for Proportional Amplifier with T Network Model for Control

| Frequency $\frac{w_+}{v_+}$ | Node 1 | | Node 2 | |
|---|---|---|---|---|
| | Amplitude Gain | Phase (Degree) | Amplitude Gain | Phase (Degree) |
| 1.00000-03 | 9.03214-01 | -4.18349+00 | 9.03411+00 | -4.30954+00 |
| 1.12202-03 | 9.04068-01 | -4.69870+00 | 9.04317+00 | -4.84014+00 |
| 1.25893-03 | 9.05144-01 | -5.27875+00 | 9.05458+00 | -5.43746+00 |
| 1.41254-03 | 9.06500-01 | -5.93237+00 | 9.06896+00 | -6.11047+00 |
| 1.58489-03 | 9.08209-01 | -6.66972+00 | 9.08708+00 | -6.86957+00 |
| 1.77828-03 | 9.10364-01 | -7.50267+00 | 9.10994+00 | -7.72694+00 |
| 1.99526-03 | 9.13081-01 | -8.44523+00 | 9.13876+00 | -8.69696+00 |
| 2.23872-03 | 9.16509-01 | -9.51434+00 | 9.17514+00 | -9.79679+00 |
| 2.51189-03 | 9.20835-01 | -1.07302+01 | 9.22107+00 | -1.10472+01 |
| 2.81838-03 | 9.26298-01 | -1.21178+01 | 9.27909+00 | -1.24736+01 |
| 3.16228-03 | 9.33197-01 | -1.37083+01 | 9.35242+00 | -1.41077+01 |
| 3.54813-03 | 9.41913-01 | -1.55415+01 | 9.44513+00 | -1.59899+01 |
| 3.98107-03 | 9.52923-01 | -1.76688+01 | 9.56236+00 | -1.81723+01 |
| 4.46684-03 | 9.66817-01 | -2.01585+01 | 9.71053+00 | -2.07239+01 |
| 5.01187-03 | 9.84307-01 | -2.31028+01 | 9.89742+00 | -2.37380+01 |
| 5.62341-03 | 1.00620+00 | -2.66295+01 | 1.01320+01 | -2.73432+01 |
| 6.30957-03 | 1.03326+00 | -3.09181+01 | 1.04234+01 | -3.17203+01 |
| 7.07946-03 | 1.06590+00 | -3.62736+01 | 1.07771+01 | -3.71257+01 |
| 7.94328-03 | 1.10314+00 | -4.29050+01 | 1.11857+01 | -4.39202+01 |
| 8.91251-03 | 1.14051+00 | -5.14422+01 | 1.16066+01 | -5.25853+01 |
| 1.00000-02 | 1.16587+00 | -6.23767+01 | 1.19193+01 | -6.36652+01 |
| 1.12202-02 | 1.15537+00 | -7.60303+01 | 1.18806+01 | -7.74845+01 |
| 1.25893-02 | 1.08035+00 | -9.19040+01 | 1.11912+01 | -9.35478+01 |
| 1.41254-02 | 9.35600-01 | -1.08299+02 | 9.78258+00 | -1.10161+02 |
| 1.58489-02 | 7.55681-01 | -1.23161+02 | 7.99569+00 | -1.25275+02 |
| 1.77828-02 | 5.83978-01 | -1.35388+02 | 6.27319+00 | -1.37796+02 |
| 1.99526-02 | 4.42347-01 | -1.44979+02 | 4.84476+00 | -1.47734+02 |
| 2.23872-02 | 3.33241-01 | -1.52410+02 | 3.74192+00 | -1.55580+02 |
| 2.51189-02 | 2.51389-01 | -1.58194+02 | 2.91540+00 | -1.61867+02 |
| 2.81838-02 | 1.90406-01 | -1.62733+02 | 2.30315+00 | -1.67034+02 |
| 3.16228-02 | 1.44909-01 | -1.66323+02 | 1.85301+00 | -1.71426+02 |
| 3.54813-02 | 1.10816-01 | -1.69171+02 | 1.52663+00 | -1.75344+02 |
| 3.98107-02 | 8.51331-02 | -1.71433+02 | 1.29877+00 | -1.7911C+02 |

TABLE 2

THEORETICAL RESULTS OF A THREE-STAGE GAIN BLOCK

| FREQUENCY $\frac{w+}{v+}$ | AMPLIFIER 1 | | AMPLIFIER 2 | | AMPLIFIER 3 | |
|---|---|---|---|---|---|---|
| | Ampl. Gain | Phase In Degrees | Ampl. Gain | Phase In Degrees | Ampl. Gain | Phase In Degrees |
| 1.00000-03 | 9.95141+00 | 1.23393+00 | 9.90722+01 | 2.47375+00 | 9.88467+02 | 2.58760+00 |
| 1.12202-03 | 9.93197+00 | 1.38091+00 | 9.86350+01 | 2.76921+00 | 9.85520+02 | 2.89711+00 |
| 1.25893-03 | 9.92368+00 | 1.54317+00 | 9.85380+01 | 3.09837+00 | 9.81831+02 | 3.24186+00 |
| 1.41254-03 | 9.90369+00 | 1.72386+00 | 9.81668+01 | 3.46402+00 | 9.77222+02 | 3.62515+00 |
| 1.58489-03 | 9.87956+00 | 1.92325+00 | 9.77038+01 | 3.86932+00 | 9.7147+02 | 4.05029+00 |
| 1.77828-03 | 9.84923+00 | 2.14264+00 | 9.71274+01 | 4.31715+00 | 9.64823+02 | 4.52046+00 |
| 1.99526-03 | 9.81152+00 | 2.38283+00 | 9.64120+01 | 4.81034+00 | 9.55452+02 | 5.03850+00 |
| 2.23872-03 | 9.76479+00 | 2.64414+00 | 9.55270+01 | 5.34936+00 | 9.44487+02 | 5.60666+00 |
| 2.51189-03 | 9.70710+00 | 2.92620+00 | 9.44370+01 | 5.93745+00 | 9.30994+02 | 6.22620+00 |
| 2.81838-03 | 9.63619+00 | 3.22764+00 | 9.31016+01 | 6.57210+00 | 9.14483+02 | 6.89691+00 |
| 3.16228-03 | 9.54952+00 | 3.54580+00 | 9.14754+01 | 7.25100+00 | 8.94414+02 | 7.61650+00 |
| 3.54813-03 | 9.44428+00 | 3.87627+00 | 8.95114+01 | 7.96847+00 | 8.70216+02 | 8.37990+00 |
| 3.98107-03 | 9.31748+00 | 4.21309+00 | 8.71609+01 | 8.71524+00 | 8.41329+02 | 9.17850+00 |
| 4.46684-03 | 9.16606+00 | 4.54750+00 | 8.43775+01 | 9.47774+00 | 8.07238+02 | 9.99936+00 |
| 5.01187-03 | 8.98710+00 | 4.86893+00 | 8.11237+01 | 1.02375+01 | 7.67554+02 | 1.08247+01 |
| 5.62341-03 | 8.77749+00 | 5.16477+00 | 7.73753+01 | 1.09710+01 | 7.22089+02 | 1.16314+01 |
| 6.30957-03 | 8.53669+00 | 5.42117+00 | 7.31282+01 | 1.16500+01 | 6.70943+02 | 1.23916+01 |
| 7.07946-03 | 8.26194+00 | 5.62417+00 | 6.84039+01 | 1.22428+01 | 6.14574+02 | 1.30736+01 |
| 7.94328-03 | 7.95337+00 | 5.76115+00 | 6.32537+01 | 1.27164+01 | 5.53873+02 | 1.36435+01 |
| 8.91251-03 | 7.61165+00 | 5.82246+00 | 5.77592+01 | 1.30390+01 | 4.90122+02 | 1.40680+01 |
| 1.00000-02 | 7.23837+00 | 5.80281+00 | 5.20288+01 | 1.31838+01 | 4.24980+02 | 1.43179+01 |
| 1.12202-02 | 6.83610+00 | 5.70207+00 | 4.61911+01 | 1.31321+01 | 3.60346+02 | 1.43709+01 |
| 1.25893-02 | 6.40827+00 | 5.52524+00 | 4.03847+01 | 1.28760+01 | 2.98191+02 | 1.42149+01 |
| 1.41254-02 | 5.95918+00 | 5.28162+00 | 3.47469+01 | 1.24204+01 | 2.40365+02 | 1.38499+01 |
| 1.58489-02 | 5.49405+00 | 4.98340+00 | 2.94026+01 | 1.17827+01 | 1.88401+02 | 1.32887+01 |
| 1.77828-02 | 5.01902+00 | 4.64399+00 | 2.44559+01 | 1.09916+01 | 1.43368+02 | 1.25559+01 |
| 1.99526-02 | 4.54102+00 | 4.27680+00 | 1.99839+01 | 1.00840+01 | 1.05730+02 | 1.16864+01 |
| 2.23872-02 | 4.06753+00 | 3.89432+00 | 1.60342+01 | 9.10220+00 | 7.55939+01 | 1.07223+01 |
| 2.51189-02 | 3.60614+00 | 3.50790+00 | 1.26258+01 | 8.08986+00 | 5.22867+01 | 9.70902+00 |
| 2.81838-02 | 3.16395+00 | 3.12792+00 | 9.75173+00 | 7.09898+00 | 3.49699+01 | 8.69254+00 |
| 3.16228-02 | 2.74713+00 | 2.76406+00 | 7.38287+00 | 6.13730+00 | 2.26509+01 | 7.71571+00 |
| 3.54813-02 | 2.36049+00 | 2.42548+00 | 5.47825+00 | 5.26653+00 | 1.41854+01 | 6.91598+00 |
| 3.98107-02 | 2.00726+00 | 2.12085+00 | 3.98055+00 | 4.50126+00 | 8.59822+00 | 6.02367+00 |
| 4.46684-02 | 1.68923+00 | 1.85749+00 | 2.83131+00 | 3.85867+00 | 5.04458+00 | 5.36126+00 |
| 5.01187-02 | 1.40671+00 | 1.64353+00 | 1.97049+00 | 3.34898+00 | 2.86549+00 | 4.84370+00 |
| 5.62341-02 | 1.15892+00 | 1.48262+00 | 1.34109+00 | 2.97612+00 | 1.57570+00 | 4.47971+00 |
| 6.30957-02 | 9.44197-01 | 1.37892+00 | 8.91655-01 | 2.74061+00 | 8.38214-01 | 4.27399+00 |
| 7.07946-02 | 7.60192-01 | 1.33528+00 | 5.78787-01 | 2.64102+00 | 4.40673-01 | 4.23041+00 |
| 7.94328-02 | 6.04149-01 | 1.35481+00 | 3.65778-01 | 2.67772+00 | 2.13375-01 | 4.35607+00 |
| 8.91251-02 | 4.73079-01 | 1.44287+00 | 2.24322-01 | 2.85699+00 | 1.00981-01 | 4.66705+00 |
| 1.00000-01 | 3.63931-01 | 1.61021+00 | 1.32739-01 | 3.19727+00 | 4.54468-02 | 5.14735+00 |

## 7. SUMMARY

The results of this investigation have shown that the laminar proportional amplifier offers a significant improvement over available proportional amplifiers in its gain characteristic, dynamic range, ability to be staged properly, and ability to be scaled.

A laminar proportional amplifier with a single-stage pressure gain greater than 15, a smooth gain characteristic that saturates when overdriven, and a dynamic range that exceeds 1000 has been built. This element operates properly in a Reynolds number range of 750 to 1500, based on the element depth. The amplifier performance is limited by low gain at the lower end and by flow noise at the upper end of the Reynolds number range. Within this Reynolds number range, elements have been made to operate with different working fluids such as air and hydraulic oil. Their performance characteristics are similar when the operating Reynolds number is the same.

A control volume analysis has been made to describe the dynamic response of this amplifier. The theoretical results are in good agreement with the experimental measurements. This amplifier's dynamic response has no noticable resonance and becomes overdamped when the element is overdriven in amplitude. The dynamic response of these elements depends on the average supply jet velocity and the physical size of the plan view of the element. Typical elements have response beyond 500 Hz, and some elements with 0.5-mm power nozzle widths operating at power supply pressure from 0.5 to 1.5 kPa have responses exceeding 1000 Hz. A low pressure first-stage response is typically 150 to 250 Hz for signal levels of 0.0002 kPa.

A method has been developed to stage these amplifiers to form pressure, flow, and/or power gain blocks. Using these amplifiers, a three-stage pressure gain block has been built that has a pressure gain greater than 1000, a bandwidth of 100 Hz, and a dynamic range of about 500.

In addition, because this amplifier uses a pressure field to deflect the power jet, it is possible to build a summing amplifier by summing control flows into the control pressure field.

The results of this investigation are promising and our future effort will be directed toward the refinement of the laminar proportional amplifier and the different gain blocks so that they can be readily used in many control systems where the reliability and environmental hardness of fluidic control is needed.

## LIST OF SYMBOLS

| | | |
|---|---|---|
| a, b, c | - | coefficients in quadratic equation |
| C | - | jet compliance |
| $C_D$ | - | discharge coefficient |
| $G_{po}$ | - | pressure gain at zero bias level |
| $G_p$ | - | pressure gain |
| h | - | channel height |
| K | - | bias coefficient |
| k | - | $Y_1/Y_o$ |
| L | - | inductance |
| $\ell$ | - | length |
| $\ell_1$ | - | distance between supply nozzle and edge of control nozzle |
| $\ell_2$ | - | distance between edge of control nozzle and splitter |
| $\ell_T$ | - | distance between supply nozzle and splitter ($\ell_T = \ell_1 + \ell_2$) |
| m | - | number of paralle elements in the driven stage |
| p | - | pressure |
| Q | - | flow |
| R | - | resistance |
| Re | - | $V_+h/\nu$, Reynolds number |
| s | - | Laplace operator |
| t | - | time |
| $t_+$ | - | $w_+/V_+$, characteristic time |
| $V_+$ | - | average velocity of jet at supply nozzle |
| w | - | width |
| $w_+$ | - | supply nozzle width |
| y | - | lateral displacement of jet |
| Y | - | admittance |
| Z | - | impedance |
| $\gamma$ | - | ratio of specific heat |
| $\theta$ | - | jet angle at the end of control volume |
| $\omega_a$ | - | single lead frequency |
| $\omega_b$ | - | lag frequency |
| $\omega_c$ | - | resonant frequency |
| $\zeta$ | - | damping ratio |

Subscripts

0 - zero jet deflection
1 - control volume or side 1
2 - vent or side 2
av - average
c - capacitive
e - entrained
i - input
j - supply jet
n - n-th stage
o - output
r - ratio
T - total
v - vent
+ - supply